

**Aus dem Institut für Physiologie  
der Universität Tübingen  
Abteilung Physiologie I  
Abteilungsleiter: Professor Dr. F. Lang**

**Clcn2 polymorphisms in Africans from an endemic  
malaria area**

**Inaugural-Dissertation  
zur Erlangung des Doktorgrades der Medizin  
der Medizinischen Fakultät der Eberhard Karls Universität  
zu Tübingen**

**vorgelegt von**

**Jochen Paul**

**aus Friedrichshafen**

**2006**

Dekan: Professor Dr. I. B. Autenrieth

1. Berichterstatter: Privatdozent Dr. S. M. Huber

2. Berichterstatter: Professor P. Kremsner



# Contents:

<b>1 Introduction .....</b>	<b>1</b>
<b>1.1 Malaria.....</b>	<b>1</b>
1.1.1 Life cycle .....	3
1.1.2 Clinical symptoms.....	4
<b>1.2 Infected erythrocytes.....</b>	<b>5</b>
1.2.1 New permeability pathways .....	5
1.2.2 PSAC – plasmodial erythrocyte surface anion.....	6
channel .....	6
1.2.3 Infection-Induced Outwardly Rectifying Anion .....	7
Channels .....	7
1.2.4 Alterations of the Host Erythrocyte Volume .....	9
1.2.5 ClC-2 Channels in <i>Plasmodium</i> -infected .....	10
erythrocytes.....	10
<b>1.3 ClC-2 Channel.....</b>	<b>12</b>
1.3.1 General features of Cl channels .....	12
1.3.2 Molecular genetics of ClC-2 .....	12
1.3.3 Topology of ClC channels .....	15
1.3.4 Functional properties of ClC-2.....	17
1.3.5 Physiological functions of ClC-2 channels .....	18
<b>1.4 Objectives of the study .....</b>	<b>20</b>
<b>2 Materials and Methods .....</b>	<b>21</b>
<b>2.1 Patients.....</b>	<b>21</b>
<b>2.2 Molecular biological materials and methods.....</b>	<b>22</b>
2.2.1 Polymerase chain reaction (PCR).....	22
2.2.2 Agarose gel electrophoresis of DNA.....	24
2.2.3 Sequence analysis .....	25
2.2.4 Products and kits .....	26
<b>2.3 Electrophysiological materials and methods.....</b>	<b>27</b>
2.3.1 Buffers and Solutions .....	27
2.3.2 Oocyte isolation and preparation.....	29
2.3.2 cRNA-syntheses / injection.....	30

2.3.3 Two-electrode voltage-clamp (TEVC).....	30
2.3.4 Three dimensional structural model of the CBS1 .....	32
domain of CLC-2.....	32
<b>3 Results .....</b>	<b>33</b>
<b>3.1 Molecular biology.....</b>	<b>33</b>
3.1.1 Frequency of polymorphisms .....	33
3.1.2 Polymorphic positions in the Clcn2 gene .....	35
<b>3.2 Electrophysiology.....</b>	<b>37</b>
3.2.1 Isoosmotic bath solution .....	37
3.2.2 Voltage dependence and kinetics (isoosmotic).....	40
3.2.3 Hypoosmotic cell swelling .....	44
3.2.4 Voltage dependence and kinetics (hypoosmotic).....	47
<b>3.3 Model of CLC-2 channel.....</b>	<b>52</b>
<b>3.4 Cystathionine Beta Synthase -1 domain.....</b>	<b>53</b>
3.4.1 Alignment of the CBS-domains.....	53
3.4.2 CLC-CBS-domain1 3D-model .....	54
<b>4 Discussion .....</b>	<b>55</b>
<b>4.1 Sources of error.....</b>	<b>55</b>
4.1.1 General aspects of the oocyte expression system.....	55
4.1.2 Oocytes and cRNA .....	55
4.1.3 Solutions .....	56
<b>4.2 Identification of polymorphisms .....</b>	<b>57</b>
<b>4.3 Functional characterization of polymorphisms.....</b>	<b>58</b>
<b>4.4 Influence of polymorphisms on malaria.....</b>	<b>60</b>
<b>5 Summary .....</b>	<b>61</b>
<b>6 References.....</b>	<b>63</b>
<b>7 Appendix.....</b>	<b>71</b>
<b>7.1 Acknowledgment.....</b>	<b>71</b>
<b>7.2 Curriculum Vitae.....</b>	<b>72</b>

# 1 Introduction

## 1.1 Malaria

Malaria is an infectious disease transmitted by the bite of the female Anopheles mosquito. Today approximately 40% of the world's population, mostly those living in some of the world's poorest countries, are at risk of malaria. It causes more than 300 million acute illnesses and at least 1 million deaths per year. Around 90% of these deaths occur in Africa where young children are seen as being especially at risk. According to the WHO every 30 seconds one African child is killed by Malaria (WHO, 2005). The disease is found mainly throughout the tropical and sub-tropical regions of the world.

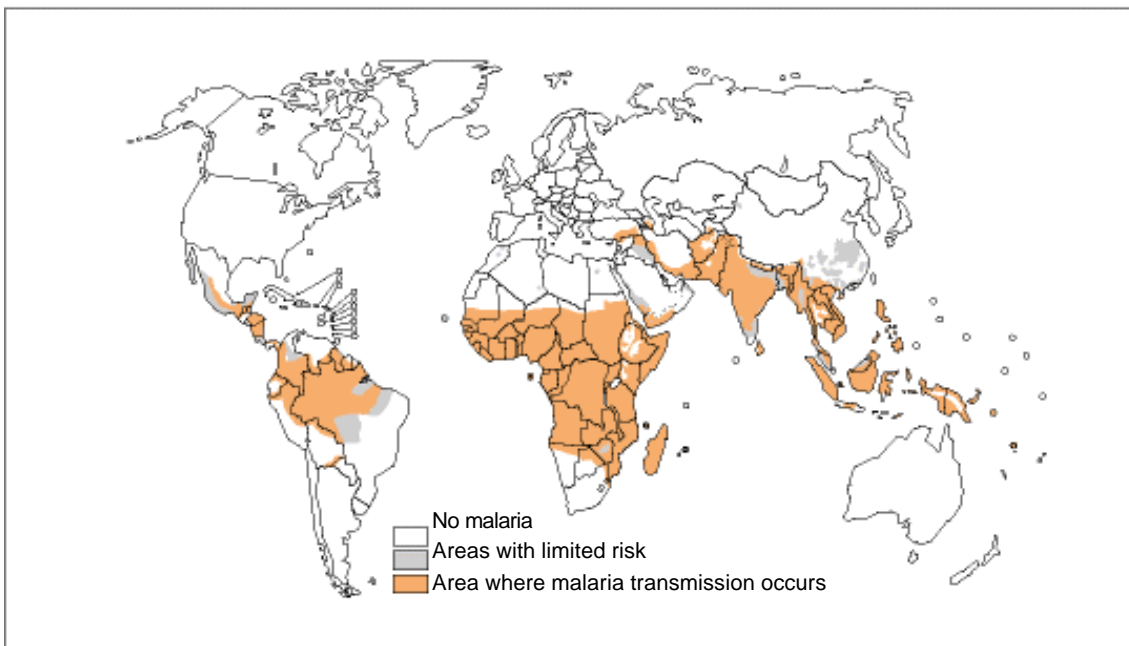


Figure 1: Malaria distribution in 2005 according to the World Health Organization ([www.who.int](http://www.who.int))

Over the last few years the situation has become even more complex because Malaria parasites have been developing unacceptable levels of resistance to one drug after another.

Malaria is caused by intracellular protozoan parasites of the genus *Plasmodium*. When an infected Anopheles mosquito takes a blood meal the parasite enters the human host. Protozoas are unicellular eukaryotic organisms which undergo a series of changes to evade detection of the immune system, infect liver hepatocytes and red blood cells (RBC) and the liver, and finally, develop into a form that infects a mosquito again when an infected person is bitten. Four species of *Plasmodium* can produce Malaria in its various forms:

- |  |                 |
|--|-----------------|
| - <i>Plasmodium falciparum</i>   | Malaria tropica |
| - <i>Plasmodium viva</i><br>(Indian sub-continent and Central America)   | Tertia malaria  |
| - <i>Plasmodium ovale</i><br>(relatively unusual outside Africa)         | Tertian malaria |
| - <i>Plasmodium malariae</i><br>(most endemic areas, sub-Saharan Africa) | Quartan malaria |

According to the WHO *P. vivax* and *P. falciparum* are the most common forms. *P. falciparum* causes the most severe and often lethal type of malaria infection. In regions of the world where malaria had been eliminated concern surrounding the spread of malaria is increasing.

Malaria, along with HIV/AIDS and Tuberculosis, is one of the major public health challenges facing the poorest countries of the world.

## 1.1.1 Life cycle

### 1.1.1.1 The asexual cycle

*Plasmodium* develops in the gut of a infected Anopheles mosquito and is passed in the saliva of the female insect. Each time an infected mosquito takes a blood meal the host's blood gets infected with sporozoites. The sporozoites circulate in the blood for about 30 minutes and then settle in the sufferer's liver where they multiply and differentiate into merozoites. This stage is known as exoerythrocytic schizogony. This phase is asymptomatic and lasts, depending on the species of *Plasmodium*, between 7 and 42 days (Hof *et al.*, 2000). In *P. vivax* and *P. ovale*, as well as in *P. malariae* infections parasites may persist in the liver for between 5 and 50 years (Renz-Polster *et al.*, 2004). The liver cells then lyse and free merozoites, passing them into the host's blood stream. By invading the host's RBCs the parasite protects itself from the host's immune system, the harmful or lethal effects of antibodies or from other cellular defence mechanisms. After entering the RBC, merozoites differentiates to trophozoites. These morphological changes of *Plasmodium* are accompanied by a progressive increase of metabolic and biosynthetic activity of the parasite within the RBC (Sherman, 1983; Kirk *et al.*, 1991). The parasite then enters the schizont stage which results in the formation of 8 to 32 daughter merozoites (*P. falciparum*). The infected erythrocytes finally rupture and release these merozoites, ready to invade new red blood cells. The duration of the cycle depends upon the species of *Plasmodium*.

### 1.1.1.2 The sexual cycle

During the intraerythrocytic schizogony the schizontes differentiate into male and female gametocytes, which are taken up by the female *Anopheles* mosquito with the blood meal. In the mosquitoes gut the gametocytes fuse to form a zygote which matures and produces sporozoites. These sporozoites are spread via the salivary gland and the *Anopheles* mosquito can now initiate the cycle again.

### 1.1.2 Clinical symptoms

About one third of infections with *Plasmodiums* are forms of mild malaria. These ones are caused by *P. vivax* , *P. ovale* and *P. malariae*. Symptoms include fatigue caused by fever, recurrent chills, and haemolytic anaemia.

Two third of the cases are forms of severe malaria caused by *P. falciparum*. Intense headaches, pain in the joints, splenomegaly and hepatomegaly are accompanied by complications like cerebral malaria, intravascular haemolysis (bilious fever), glomerulonephritis caused by immune complexes, leuko- and thrombopenia, hypoglycaemia (especially children) and oedema of lung (Renz-Polster *et al.*, 2004).

## 1.2 Infected erythrocytes

### 1.2.1 New permeability pathways

Before infection, the human RBC is little more than a bag of haemoglobin with limited nutritional needs. Survival and replication of *Plasmodium falciparum* is highly dependent on a sufficient supply of nutrients and adequate disposal of metabolic wastes by the host cell. As a consequence, the intraerythrocytic parasite must induce new transport pathways across the plasma membrane of the host RBC (Ginsburg & Kirk, 1998; Kirk, 2001). These so-called New Permeability Pathways (NPP) become apparent about 12-15 h post-invasion of the merozoite into the RBC and increase markedly up to a plateau at about 36 h post-invasion (Staines *et al.*, 2001). The membrane of RBCs infected with malaria parasites is highly permeable to a large variety of solutes, including anions, carbohydrates, amino acids, nucleosides, organic and inorganic cations and small peptides (Ginsburg & Stein, 2004).

The necessity of the NPP for the survival of *Plasmodium falciparum* is illustrated by the fact that in vitro parasite growth is blocked by several inhibitors of these pathways (Ginsburg & Kirk, 1998; Kirk, 2001). The NPP are inhibited by a wide molecular range of drugs. Among them are furosemide, phlorizin, niflumic acid, NPPB [5-nitro-2-(3-phenylpropylamino)benzoic acid], and glibenclamide (Kutner *et al.*, 1987; Kirk *et al.*, 1993; Kirk *et al.*, 1994; Kirk & Horner, 1995).

These NPPs are of high clinical interest. First, as possible drug targets for antimalarial chemotherapy and second as routes capable of delivering drugs from the blood to the intraerythrocytic parasite (Kirk, 2004).

According to these NPP infection challenges cell volume constancy of the host erythrocyte requiring enhanced activity of cell volume regulatory mechanisms. Huber *et al* concluded that activation of host CIC-2 channels participates in the altered permeability of *Plasmodium*-infected erythrocytes (Huber *et al.*, 2004).

At present, neither the origin nor the molecular identity of the New Permeability Pathways is defined. In principle, the pathways could be generated by endogenous RBC proteins or by parasite-encoded xenoproteins that are exported and trafficked into the RBC membrane.

## 1.2.2 PSAC – plasmodial erythrocyte surface anion channel

In 2000 Desai et co-workers identified by on-cell single channel recording an anion channel with low unitary conductance (20 pS chord conductance in symmetrical 1.1 M Cl<sup>-</sup>) on the RBC membrane of trophozoite-stage infected human RBCs (Desai *et al.*, 2000). 1000–2000 functional copies were estimated to be present per infected RBC. This channel type has been called the plasmodial erythrocyte surface anion channel (PSAC) because it was not observed in uninfected RBCs (Desai *et al.*, 2000). PSAC shows highly voltage-dependent single channel gating with higher open probability at hyperpolarizing voltages. PSAC is inhibited by furosemide (125 μM) added to the pipette solution and shows a complex fast-flickering gating with bursts of openings with mean open times of 0.5 ms (Desai *et al.*, 2000). Desai et al. have concluded that PSAC is the predominant conductive Cl<sup>-</sup> pathway in the infected RBC membrane (Desai *et al.*, 2000).

Afterwards, Desai et al. extended a mathematical model of osmotic fragility (Saari & Beck, 1974; Beck & Saari, 1977) in isosmotic sorbitol solutions for *Plasmodium falciparum*-infected human RBCs (Wagner *et al.*, 2003). As a result, the model confirms the previous suggestion that PSAC is generating the predominant Cl<sup>-</sup> conductance in *Plasmodium falciparum* infected human RBCs (Desai *et al.*, 2000).

According to the functional significance the most striking evidence for a functional role of PSAC channels in the promotion of intraerythrocytic parasite growth comes from the observation that a number of drugs (phlorizin, glibenclamide, NPPB, furosemide, and derivatives thereof (Kutner *et al.*, 1987; Silfen *et al.*, 1988; Kirk *et al.*, 1993; Kirk & Horner, 1995) inhibit PSAC channels and impair the in vitro growth of malaria parasites. It remains unclear, however, whether the antiparasitic effect of these compounds can be attributed to their effect on the PSAC channel. Up to now the PSAC in the host RBC membrane has not been identified on molecular level and the final proof for such a function requires the molecular identification/cloning of the channel.

## 1.2.3 Infection-Induced Outwardly Rectifying Anion

### Channels

Patch-clamp studies by Huber et al in addition to a PSAC-like conductance (Huber *et al.*, 2004) have revealed an additional anion conductance to be active in late trophozoite-infected mouse and human erythrocyte (Huber *et al.*, 2002; Huber *et al.*, 2004). By modifying the recording conditions (using negative holding potentials and transferring the infected RBCs directly from the culture medium into the patch-clamp superfusion without enrichment or washing steps) this conductance became apparent (Staines *et al.*, 2003). A time-dependent inactivation of the inward current and a variable time-dependent activation of the outward current resulting in an outwardly rectifying (OR) voltage relationship of the steady state current was shown. The OR channels (*Plasmodium falciparum*-induced) are generated by DIDS (4,4'-diisothiocyanatostibene- 2,2'-disulphonic acid) sensitive endogenous RBC anion channels most probably. They show low spontaneous activity in non-infected RBCs but may become active under oxidative stress of RBCs (Huber *et al.*, 2002). Osmotic RBC shrinkage or swelling does not modify these (Duranton *et al.*, 2004; Huber *et al.*, 2004). They are not dependent on ATP in the pipette solution or glucose in the bath and are active at room temperature (Duranton *et al.*, 2003). The OR channels share some common features with cell-volume independent anion channels in embryonic epithelial cells, as rectification, time-dependent activation/inactivation, permselectivity, and DIDS-sensitivity (Huber & Horster, 1996, 1998).

Most infected RBCs analyzed by Huber et al (Huber *et al.*, 2004) exhibited both OR and PSAC-like currents. Spontaneous OR channel activity in non-infected unstimulated RBCs occurred with similar low frequency as that of PSAC-like channels. That clearly indicates the infection-stimulated activation of OR channels (Huber *et al.*, 2002; Duranton *et al.*, 2004).

OR channels could be experimentation-induced modifications of the PSAC channels. The PSAC-like inwardly rectifying currents observed by Huber et al. (Huber *et al.*, 2004) could belong to a further type of anion channels such as CIC-2.

The putative PSAC-mediated inwardly rectifying whole-cell currents could result from the activities of both channels. In most studies on infected human RBCs the lack of OR appearance (Desai *et al.*, 2000; Egee *et al.*, 2002; Verloo *et al.*, 2004) could be attributed to the fact that these studies preferred to work at 0 mV holding potential. This is close to the physiological membrane potential of late trophozoite-infected RBCs. The activities of PSAC and OR channels might as well depend on each other. This could explain the partially similar pharmacology found for OR and PSAC channels.

### **1.2.4 Alterations of the Host Erythrocyte Volume**

With parasite development  $K^+$  and  $Na^+$  leakage through the RBC membrane increases. The induced cation leakage initially hyperpolarizes the membrane potential since the  $K^+$  permeability exceeds that for  $Na^+$  by a factor of about 2. This leads to the loss of KCl and water and to an intermediate shrinkage of the parasitized RBCs (Staines *et al.*, 2001; Lew *et al.*, 2003). A further increase in cation permeability during later parasite development, is paralleled by a decline of  $Na^+/K^+$  pump activity. This is followed by the replacement of the cytosolic  $K^+$  ions by  $Na^+$  and the collapse of the chemical  $Na^+$  and  $K^+$  gradients across the RBC membrane. The membrane potential depolarises due to the loss of these gradients. An induction of the net uptake of NaCl and water results in colloid osmotic RBC swelling (Tanabe *et al.*, 1986; Staines *et al.*, 2001). Trophozoite/schizont-infected RBCs reach the lytic volume and haemolyse colloid osmotically prior to maturation of the parasite. The parasite and the host cell prevent this premature haemolysis. The parasite lowers the colloid concentration in the host RBC cytosol by excess digestion of haemoglobin while the host cell exports the haemoglobin-derived amino acids to the extracellular space (Lew & Hockaday, 1999; Lew *et al.*, 2003; Lew *et al.*, 2004). Up to 65% of the host cell's haemoglobin is digested by the intraerythrocytic parasite but only up to about 16% of the amino acids are utilized (Rudzinska *et al.*, 1965; Krugliak *et al.*, 2002). The New Permeability Pathways are used to release the haemoglobin-derived amino acids into the blood plasma (Krugliak *et al.*, 2002). By the export of organic osmolytes the RBC volume expansion is regulated and the host RBC haemolysis is delayed until the end of parasite development. Taken together the function of the New Permeability Pathways is in sharp contrast to those of the anion channels in non-infected RBCs.

In contrast to nucleated cells non-infected RBCs do not utilize anion channels (Hamill, 1983; Egee *et al.*, 1997; Egee *et al.*, 1998; Egee *et al.*, 2000) for regulatory volume decrease but lower their volume by KCl co transport activity (Ellory & Hall, 1988). Accordingly, hypo-osmotic cell-swelling does not activate anion channels during whole-cell recording in non-infected RBCs (Huber *et al.*, 2001).

## 1.2.5 CIC-2 Channels in *Plasmodium*-infected erythrocytes

Huber et al. tested malaria-induced activation of cell volume-sensitive ion channels in the host membrane by measuring whole-cell currents of *Plasmodium falciparum* infected human RBCs and of *Plasmodium berghei* infected mouse RBCs (Huber et al., 2004). Cell-shrinkage inhibits and cell swelling activates a fraction of the whole-cell inward current and in both species. This volume-sensitive current fraction is anion-selective and amounts to almost 50% of the total inward current in swollen infected cells. Swelling of unstimulated non-infected human RBCs, however, does not activate any appreciable current in human and mouse RBCs (Duranton et al., 2004; Huber et al., 2004). This data clearly indicates that malaria infection is necessary responsible for the activation of the current fraction by cell-swelling.

The cell swelling-sensitive current fraction of infected mouse and human RBCs activates time-dependently upon hyperpolarization. It exhibits an inwardly rectifying current voltage relationship and is  $ZnCl_2$  sensitive but NPPB-insensitive (Huber et al., 2004). These properties resemble those of the ubiquitously expressed, swelling-activated  $Cl^-$  channel CIC-2 (Grunder et al., 1992; Thiemann et al., 1992; Jentsch et al., 1995; Clark et al., 1998; Bosl et al., 2001; Nehrke et al., 2002).

*Plasmodium berghei*-infected RBCs from wildtype ( $Clcn2^{+/+}$ ) and  $Clcn2^{-/-}$  mice have been tested to specify the role of CIC-2 (Huber et al., 2004). For this purpose cell-volume changes and whole-cell currents have been compared.  $Na^+$ -and  $K^+$ -permealized infected RBCs from  $Clcn2^{-/-}$  mice shrank significantly slower than infected RBCs from wildtype mice when suspended in  $NaCl$  free solution containing NPPB (100  $\mu$ M) to inhibit PSAC channels. In infected RBCs from  $Clcn2^{-/-}$  mice no cell volume-sensitive current fraction was measurable. Finally, the  $Clcn2^{-/-}$ -dependent current fraction of swollen mouse RBCs exhibited absolute current values, inward-rectification, and time-dependent activation (at hyperpolarizing voltages) identical to the  $ZnCl_2$  (1 mM)-sensitive current fraction (Huber et al., 2004). Together, this data demonstrates the

presence of ClC-2-mediated anion currents in *Plasmodium*-infected human and mouse RBCs.

According to the functional role of ClC-2, deficiency may impair cell volume regulation of infected RBCs leading to an increase in host volume. Huber et al. have tested this possibility by studying cell volume by FACS forward scatter of RBCs drawn from *P. berghei*-infected *Clcn2*<sup>-/-</sup> and wildtype (*Clcn2*<sup>+/+</sup>) mice (Huber *et al.*, 2004). As a result non-infected and parasitised cells from infected *Clcn2*<sup>-/-</sup> mice, exhibited a significantly higher forward scatter than the corresponding wildtype RBC groups. Further experiments studying the effect of ClC-2 inhibition by ZnCl<sub>2</sub> indicate a significant increase in forward scatter of infected wildtype RBCs but not of non-infected wildtype or non-infected and infected *Clcn2*<sup>-/-</sup> RBCs. Thus inhibition of ClC-2 increases cell volume only in parasitized RBCs, suggesting the functional significance of ClC-2 in the cell volume maintenance of the infected host RBCs (Huber *et al.*, 2004).

## **1.3 CIC-2 Channel**

### **1.3.1 General features of Cl<sup>-</sup> channels**

Cl<sup>-</sup> channels reside in the plasma membrane as well as in intracellular organelles. Their functions range from cell volume regulation and ion homeostasis to transepithelial transport and regulation of electrical excitability. Various inherited diseases (i.e. cystic fibrosis, myotonia congenita and Dent's disease) illustrate their physiological roles. There are three well established molecularly distinct Cl<sup>-</sup> channel families (CLC, CFTR, and ligand-gated GABA and glycine receptors)(Jentsch *et al.*, 2002). CIC-2 is a member of the CLC family.

### **1.3.2 Molecular genetics of CIC-2**

The human *Clcn2* gene encoding the voltage gated chloride channel CIC-2 is located on chromosome 3q26. It comprises of 24 exons which were first sequenced by Thiemann *et al.* in 1992 (Thiemann *et al.*, 1992; Cid *et al.*, 1995).

From a population living in a malaria-endemic area in Gabon (Africa) all 24 *Clcn2* exons were sequenced. Seven amino acid exchanges (P48R, R68H, G199A, R646Q, S661T, R725W, R747H) were identified in low frequency (1-4/31 or 10/80) in the African but not in a Caucasian control group. The polymorphism S668T appeared in both groups. Two amino acid exchanges (R73A, E718D) were identified in low frequency (1/10) in the Caucasian control group only.

### 1.3.2.1 Clcn2 gene

The Clcn2 gene comprises of 24 exons or coding regions. These regions are illustrated yellow in the model of the Clcn2 gene (Figure 2). In five of the coding regions (red exons) mutations were found. The mutations which resulted in an amino acid exchange are named in the model.

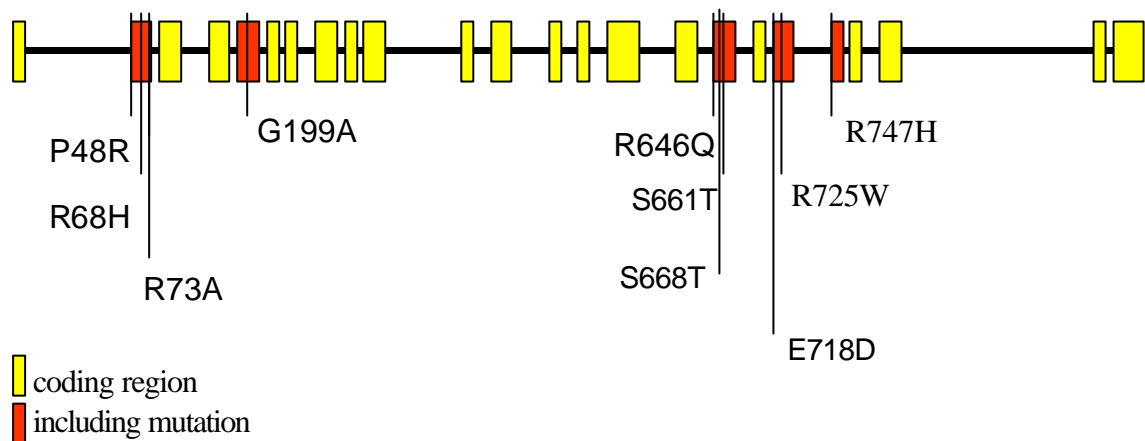
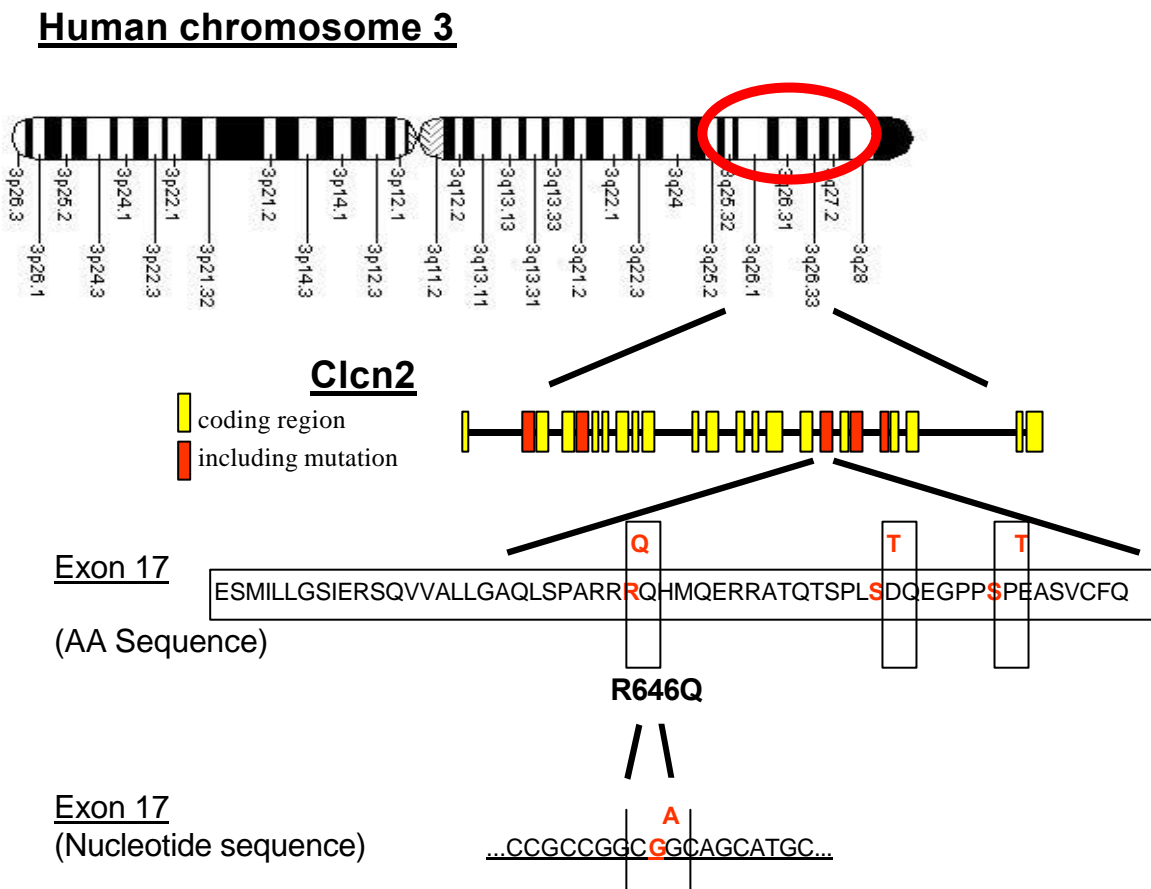


Figure 2: Mutations resulting in an amino acid exchanges found in Clcn2 gene

### 1.3.2.2 Example for Polymorphism R646Q

Figure 3 is illustrating a nucleotide sequence exchange in red (guanine to adenine) on the bottom. This exchange is leading to the amino acid mutation (Arg to Gln) on position 646 (R646Q). This exchange is located on exon 17 of the Clcn2 gene with is located on the human chromosome 3 (top).



**Figure 3:** Exchange in the nucleotide sequence (G to A) leading to amino acid exchange R646Q (R to Q) in exon 17 on chromosome 3

### 1.3.3 Topology of CLC channels

The previous analysis of CLC topology by various biochemical methods yielded a confusing picture. Now the recently identified crystal structure of CLC channels gives a definitive picture of the molecular structure of bacterial CLC proteins (Dutzler *et al.*, 2002). It reveals the presence of 18  $\alpha$ -helices that exhibit a complex topology (Fig. 4). The entire channel with two identical sub-units is shaped like a rhombus. The pore is not formed at the interface between the two rather each sub-unit forms its own pore and selectivity filter. The core structure of a CLC channel sub-unit is composed by 18  $\alpha$ -helices. Many of the helices do not qualify as classical “transmembrane helices” as they do not cross the membrane (Dutzler *et al.*, 2002; Jentsch *et al.*, 2002). Membrane topology model of CLC-2 is based on structure of *S. typhimuriun* (Dutzler *et al.*, 2002).

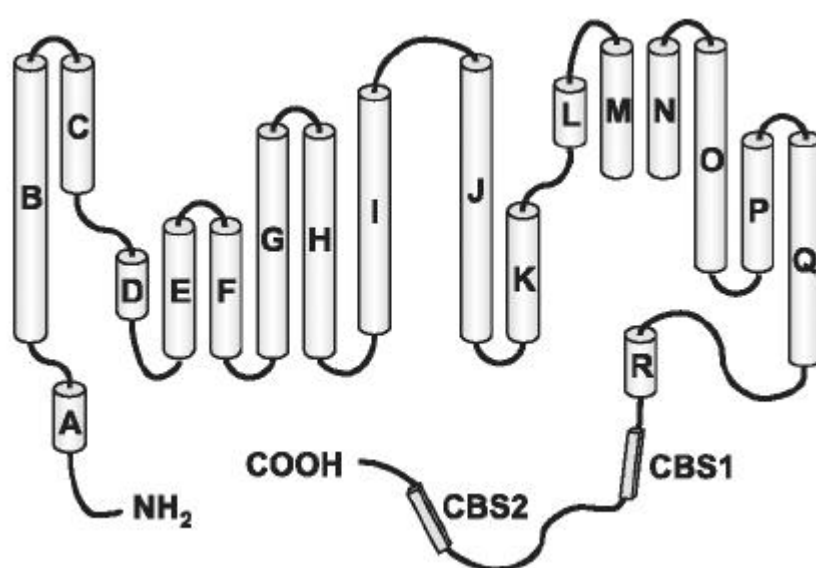


Figure 4: Model from Haug *et al.*: Mutations in Clcn2 encoding a voltage-gated chloride channel are associated with idiopathic generalized epilepsies (Haug *et al.*, 2003).

A detailed biophysical analysis by Miller *et al.* showed the “double-barrel” model of CLC-0, with two identical pores apparent (Miller & Schnellmann, 1994). These pores can be gated separately by a fast process (time constants within the 10-

ms range) and open the channel upon depolarisation. A common “gate” closes both pores at the same time. This gate is opened by hyperpolarization and is very slow (within the 10 s to minute range). This leads to long closed periods that separate the bursts of channel opening. The three-dimensional crystal structure reveals that the CIC channel is a homodimer and each sub-unit within the dimer forms its own ion conduction pore. Both of the sub-units interact at a broad interface (Dutzler *et al.*, 2002).

The protein segments that line the pores of the CIC channel are difficult to identify.

According to Jentsch *et al.* (Jentsch *et al.*, 2002) the D3-D5 region probably plays an important but poorly understood role in gating and permeation. It seems likely that several other regions of the protein may contribute to the formation of the pore as well (Jentsch *et al.*, 2002).

Most CIC protein that could be expressed functionally showed voltage-dependent gating. CIC-2 opens in response to hyperpolarization. This can be modulated by acidic extracellular pH and cell swelling. Jentsch *et al.* suggested that the region between D7 and D8 is involved in the binding of an N-terminal “ball” domain (Jentsch *et al.*, 1999).

### 1.3.4 Functional properties of CIC-2

The CIC-2 channel can be activated by hyperpolarization, (Thiemann *et al.*, 1992) cell swelling (Grunder *et al.*, 1992) and extracellular acidification (Jordt & Jentsch, 1997). Its mRNA was detected by Northern analysis at different levels in every tissue and cell line examined (skeletal, heart, brain, lung, kidney, pancreas, stomach, intestine, liver) by Thiemann *et al.* (Thiemann *et al.*, 1992). The halide selectivity sequence of CIC-2 is  $\text{Cl} > \text{Br} > \text{I}$  (Furukawa *et al.*, 1998). In *Xenopus* oocytes (Furukawa *et al.*, 1998) as well as in transfected mammalian or insect cells (Schwiebert *et al.*, 1998) CIC-2 currents activate slowly upon hyperpolarization. In oocytes, even at  $\sim 180$  mV the activation of CIC-2 does not saturate and needs more than 20 s to reach steadystate (Thiemann *et al.*, 1992).

The activation of CIC-2 by cell swelling induced by hypotonicity, either in *Xenopus* oocytes (Grunder *et al.*, 1992) or in other cells (Schwiebert *et al.*, 1998) suggested that it might be involved in regulatory volume decrease (Grunder *et al.*, 1992).

When expressed either in *Xenopus* oocytes (Furukawa *et al.*, 1998) or in mammalian cells (Schwiebert *et al.*, 1998) lowering extracellular pH also activates CIC-2. By raising extracellular pH above 7.4 it can be closed again suggesting that extracellular pH is an important physiological regulator of this channel (Jentsch *et al.*, 2002).

### 1.3.5 Physiological functions of CIC-2 channels

Hyperpolarization-activated Cl<sup>-</sup> currents superficially resembling CIC-2 channels have been observed in various tissues and cells, including neurons (Clark *et al.*, 1998), glial cells (Nobile *et al.*, 2000), choroid plexus epithelial cells (Kajita *et al.*, 2000), osteoblasts (Chesnoy-Marchais & Fritsch, 1994), pancreatic acinar cells (Carew & Thorn, 1996), salivary gland cells (Komwatana *et al.*, 1994), Leydig cells, Sertoli cells (Bosl *et al.*, 2001) and T84 colonic epithelial cells (Fritsch & Edelman, 1996). It remains, however, difficult to prove that these currents are CLC-2 mediated.

T84 colonic epithelial cells express relatively high levels of CIC-2 (Thiemann *et al.*, 1992). CIC-2 like currents were identified in their kinetic of voltage activation, Cl<sup>-</sup> > Br<sup>-</sup> > I<sup>-</sup> selectivity and pharmacology (Fritsch & Edelman, 1996). CIC-2 might contribute to transepithelial Cl<sup>-</sup> transport according to its localisation to apical cell borders of native intestinal epithelia (Gyomory *et al.*, 2000). CIC-2 was also detected by Immunocytochemistry in apical membranes of the fetal lung. Cl<sup>-</sup> and fluid secretion are important for fetal lung development and CIC-2 might be involved (Murray *et al.*, 1995).

In conclusion CIC-2 seems to be an interesting target for the treatment of cystic fibrosis to compensate for the defective CFTR chloride channel (Jentsch *et al.*, 1999). As mentioned above CIC-2-like currents are present in glia (Nobile *et al.*, 2000) and neurons (Clark *et al.*, 1998). In the brains of adult rats CIC-2 was localised close to inhibitory synapses by Immunoelectron microscopy. It is distributed to cell bodies, dendrites of neurons and astrocytes as revealed by immunocytochemistry (Sik *et al.*, 2000). Sik *et al.* suggested that CIC-2 might be used to deliver or siphon Cl<sup>-</sup> to layers with intense GABA-ergic transmission because the immunoreactivity was concentrated at contact layers of blood vessels and close to inhibitory synapses (Sik *et al.*, 2000). In conclusion a loss of CIC-2 might result in neuronal hyperexcitability. Related to this neuronal hyperexcitability is a common idiopathic generalized epilepsy for which a susceptibility locus was mapped to human chromosome 3q26 (Sander *et al.*,

2000). This locus is close to the human gene encoding CIC-2 (Protopopov *et al.*, 1996).

Bösl *et al.* (Bosl *et al.*, 2001) disrupted the *Clcn2* gene in mice to elucidate the physiological functions of CIC-2. The *Clcn2*<sup>-/-</sup> mice did not support the speculations summarized above. The mice showed neither a defect in lung development nor a defect in gastric acidification or did they suffer from spontaneous seizures according to the GABA response and the epilepsy susceptibility locus. Instead the mice revealed in a degeneration of photoreceptors and male germ cells that led to the total loss of both cell types in adults (Bosl *et al.*, 2001).

## 1.4 Objectives of the study

The human malaria parasite *Plasmodium falciparum* has been demonstrated to activate CIC-2 Cl<sup>-</sup> channels. This activation of CIC-2 has a functional relevancy in cell volume regulation. The intracellular growth of the parasite is significantly influenced by the regulation of host cell volume. If so, polymorphisms of the Clcn2 gene with a functional relevancy might have an influence in the development of the parasite and therefore course of the malaria disease.

The present work has been performed to answer the following questions:

- 1) Are there polymorphisms of the Clcn2 gene in a Malaria-endemic area (Gabon, Africa)? What is their frequency compared to a Caucasian control group?
- 2) Do the Clcn2 polymorphisms result in altered CIC-2 channel functions?
- 3) Does an altered CIC-2 channel function influence the course of Malaria infection?

## 2 Materials and Methods

### 2.1 Patients

In cooperation with PD Dr. Jürgen Kun and Andrea Weierich (Department of Parasitology, University of Tübingen) 24 exons of *Clcn2* in Africans (n= 35-80) from a population living in a malaria-endemic area in Lambaréné, Gabon, were sequenced. The area is hyperendemic for malaria and the transmission is high (Sylla *et al.*, 2000). Patient samples were either from a combination therapy trial (Kun *et al.*, 1999) or from a longitudinal survey to evaluate immunological effects of malaria (Kun *et al.*, 1998). Ethical clearance for these trials was given by the ethics committee of the International Foundation of the Albert Schweitzer Hospital. In addition, the *Clcn2* gene of a Caucasian control group (n = 10-191) was sequenced. This blood from anonymous donors of the the blood bank, University of Tübingen, was also provided by the Department of Parasitology. PCR amplification and sequencing of exon 17 was performed by myself while all other exons were analyzed by PD Dr. Jürgen Kun and Andrea Weierich.

## 2.2 Molecular biological materials and methods

### 2.2.1 Polymerase chain reaction (PCR)

DNA was purified from 200 µl of blood using the Qiagen blood kit (Qiagen, Hilden, Germany). Exons were amplified either alone or in combination with neighboring exons. Primer sequences for DNA analyses of Clcn2 exons are given in table 1.

Table 1: Primer sequences for DNA analyses of Clcn2 exons

	Forward	reverse	Seq-Primer
Exon1	940F: ggagccgagtgccaggacaga	1372R: tgctgagacttgggcccaggt	
Exon2-3	3298F: ttcccactcagcccacacac	3873R: ctccatgtctagacgagtggtgc	3583R: ccccatcagcagctctaag
Exon4-8	4097F: tatcagcgtggtccactggc	5167R: ccctacctggcaccatctcg	4644R2: gcttgcgatatgcacaaaa gg 4544F2: agtcctcctggtggaaga
Exon9	5167F1: cgagatggtgccaggtaggg	5315R1: tcctctctgataccccagc	
Exon10	5315F: gctgggggatcagagagga	5548R: cctgacctactgtggcccttat	
Exon11-12	6630F: ctcagccctgagatatgcga	7163R: aggtgcttagaagggaagct	
Exon13-14	7412F: ccacctgatcagcaggtagact	8436R: atctaggatgccctctgccct	8008R: caccagagtctcgaccctg t
Exon15	8107F: ttgtggagggtctctgggac	8436R: atctaggatgccctctgccct	
Exon16-17	8583F: atggatgggctctggagccct	9521R: agggtctggcagggactctaag	8620F: atggcaatgctctgggacc t
Exon18	8583F: atggatgggctctggagccct	9521R: agggtctggcagggactctaag	9500R: tggatctcagtagcttgct gagg
Exon19-22	9607F: ctttcctggtcctctcccaa	10530R: gaccaagatccccactgtgtcc	
Exon23-24	15395F: tgccctgtcatttagagctg	15933R: atgcacattctgggctgac	

The PCR consists of three steps (1-3) and the cyclical repetition of these steps. By heating double-stranded DNA to temperatures between 90°C and 100°C single stranded DNA is produced (1). To initiate synthesis DNA polymerase needs a small region of double-stranded DNA. By supplying oligonucleotide

primers that anneal to the template at defined points at temperatures depending on the DNA sequence of the primers starting points can be specified (2). Both DNA strands can serve as templates for DNA synthesis at 70°C by providing the adequate primers. New DNA sequences are synthesized by the polymerase (3). The DNA molecules are copies of the DNA sequence between the primers. The DNA strands are heated again to separate the original and new synthesized strands which are now available for the next cycle (Saiki *et al.*, 1988).

### 2.2.1.1 PCR components

Substance	Volume
10xPCR-Buffer	5 µl
dNTP [25mM]	0.3 µl
Taq	0.2 µl
Primer (8583F) [10µM]	2 µl
Primer (9521R) [10µM]	2 µl
DNA	1.5 µl
H <sub>2</sub> O	39 µl

### 2.2.1.2 PCR program

STEP	TEMPERATUR	TIME	CYCLES
Pre-heating	94°C	1 min	1 cycle
Denature	94°C	30 sec	
Anneal Primers	64.5°C	30 sec	35 cycles
Elongation	72°C	60 sec	
Final elongation	72°C	10 min	1 cycle

Figure 6: Program used for PCR

## 2.2.2 Agarose gel electrophoresis of DNA

Gel electrophoresis with 1% agarose gel was used to control the amplification of the expected 938 bp DNA sequence. After purification it was used again to estimate the DNA concentration of the PCR product.

The buffer system employed was 1×TBE buffer (see below).

### 10x TBE buffer

Substance	Concentration
Tris	1 M
Borat	860 mM
EDTA	20 mM

### 1% agarose gel

Agarose	1.5g
1×TBE	150ml

## 2.2.3 Sequence analysis

The PCR products to be sequenced were controlled on a 1% agarose gel as described above for amount and integrity. Afterwards the PCR products were purified with E.Z.N.A. Cycle-Pure Kit: DNA sequencing was performed by the chain termination method (Sanger *et al.*, 1977) with the chemistry described by ABI Biosystems (Foster City, CA).

50  $\mu$ l of PCR product was mixed with 200  $\mu$ l of CP-buffer and centrifuged at 10000 x g for one min. Then 750  $\mu$ l of DNA wash buffer was added and centrifuged at 10000 x g for one min again. This step was repeated once. Afterwards the PCR product was dried by centrifuging at 10000 x g for two mins. To elute the DNA 50  $\mu$ l of sterile distilled water was added and centrifuged at 10000 x g for one min.

The purified PCR products were controlled on a 1% agarose gel and the DNA concentration was estimated according to a standard.

Cycle-PCR was performed by using x  $\mu$ l of PCR products according to their DNA concentration (between 0.5 $\mu$ l and 4 $\mu$ l). H<sub>2</sub>O was added to a total reaction volume of 50  $\mu$ l.

### 2.2.3.1 Cycle PCR components

Substance	Volume
Big Dye	1 $\mu$ l
Buffer	2 $\mu$ l
Primer (9500R)	0.5 $\mu$ l
PCR product	x $\mu$ l
H <sub>2</sub> O	46.5-x $\mu$ l

### 2.2.3.2 Cycle PCR program

STEP	TEMPERATURE	TIME	CYCLES
Denature	96°C	15 sec	
Anneal Primers	50°C	30 sec	25 cycles
Elongation	60°C	240 sec	

Figure 7: Cycle PCR program

After Cycle-PCR the cycle-PCR products were purified with PERFORMA DTR V3 96-Well Short Plates.

DNA sequencing was completed on an ABI 3100 Genetic Analyser (Applied Biosystems, Foster City, USA) by A. Weierich and S. Grummes (Department of Parasitology, University of Tübingen).

### 2.2.3.3 Site-directed mutagenesis

Site-directed mutagenesis and cloning of the *Cln2* cDNA into the oocyte expression vector was performed by Andrea Weierich (Department of Parasitology, University of Tübingen).

## 2.2.4 Products and kits

Product	Company
Taq polymerase and buffers	QIAGEN
Primers	OPERON
DNA markers	BioLabs
Big Dye Terminator kit	Applied Biosystems
E.Z.N.A. Cycle-Pure Kit:	PeqLab

Figure 8: Products and kits used for experiments

## 2.3 Electrophysiological materials and methods

### 2.3.1 Buffers and Solutions

#### ND 96 (basic solution)

Substance	Concentration
NaCl	96 mM
KCl	2 mM
CaCl <sub>2</sub>	1.8 mM
MgCl <sub>2</sub>	1 mM
Tris-HEPES *	5 mM

\*Tris-HEPES is Tris-(Hydroxymethyl)-aminomethan-N-hydroxyethylpiperazin-N'-2-ethan-sulfonat (pKs 7.4) and serves as a buffer

#### OR-2 solution (Ca<sup>2+</sup>-free)

Substance	Concentration
NaCl	96 mM
KCl	2 mM
MgCl <sub>2</sub>	1 mM
Tris-HEPES *	5 mM

#### ND96 storage solution (ND96 + antibiotics)

Substance	Concentration
NaCl	96 mM
KCl	2 mM
CaCl <sub>2</sub>	1.8 mM
MgCl <sub>2</sub>	1 mM
Tris-HEPES *	5 mM
Sodiumpyruvat	2.5 nM
Theophyllin	0.5 mM
Gentamycin	50 µg/l

### Isosmotic ND48 + sucrose solution

Substance	Concentration
NaCl	48 mM
KCl	2 mM
CaCl <sub>2</sub>	1.8 mM
MgCl <sub>2</sub>	1 mM
Sucrose	96mM
Tris-HEPES *	5 mM

### Hyposmotic ND48 solution for cell swelling

Substance	Concentration
NaCl	48 mM
KCl	2 mM
CaCl <sub>2</sub>	1.8 mM
MgCl <sub>2</sub>	1 mM
Tris-HEPES *	5 mM

### 2.3.2 Oocyte isolation and preparation

Oocytes were isolated from female *Xenopus laevis* frogs by partial ovariectomy under tricaine (3-aminobenzoic acid ethyl ester) anesthesia (0.2 % for 5-10 min).



Figure 8: *Xenopus laevis*

A small incision was made in the abdomen and a lobe of ovary was removed. The removed tissue was manually dissected into small pieces of a couple of oocytes each using small forceps. Afterward the oocytes were washed for 20 min in  $\text{Ca}^{2+}$ -free hypotonic medium (OR-2 solution) to remove blood and damaged tissue. Oocytes were then defolliculated by treatment with 2 mg/ml collagenase (Worthington type I) in  $\text{Ca}^{2+}$ -free hypotonic solution for 2 – 3 hours with gentle agitation at room temperature. The oocytes were periodically checked and the digestion terminated when the oocyte follicle had been removed with minimal damage to the oocytes. Following the incubation oocytes were washed three times in  $\text{Ca}^{2+}$ -free hypotonic media, then washed three times in isotonic solution (ND96). Stage V-VI oocytes (Dumont, 1972) were selected and maintained at 18° C in the same isotonic solution supplemented with 50 µg/ml gentamicin and 2.5 mM sodium pyruvate (ND96 storage solution).

### **2.3.2 cRNA-syntheses / injection**

The pGem-HJ plasmid DNA was linearized by SpeI digestion. cRNA was transcribed using T7 RNA polymerase (mMESSAGE mMACHINE, Ambion, Austin, TX). Precipitated cRNA was dissolved in sterile H<sub>2</sub>O and yield and quality were assessed by spectroscopy and agarose gel electrophoresis by B. Noll (Department of Physiology, University of Tübingen).

On the day of their isolation, oocytes were microinjected with 27.6 nl of sterile H<sub>2</sub>O or 27.6 nl of a cRNA solution containing 2.76 ng of cRNA from either WT (wildtyp) or one of the polymorphisms by use of a pneumatic injector. The injected oocytes were incubated at 18°C for ~48 hr to allow for expression of the protein.

### **2.3.3 Two-electrode voltage-clamp (TEVC)**

The two-electrode voltage-clamp (TEVC) technique is the most widely used electrophysiological technique for the measurement of whole cell currents through ion channels or electrogenic transporters expressed in *Xenopus* oocytes. Two glass microelectrodes were impaled into the oocytes. One electrode for recording membrane potential and the other one as a current-delivering electrode. Both electrodes were filled with 3 M KCl. The membrane potential electrode was connected to a Geneclamp 500 amplifier (Axon Instruments, Foster City, CA, USA) where the signal is compared to the voltage clamp command given by a generator. The highly amplified difference of these signals is applied as a current through the current-delivering electrode across the membrane and to the bath-grounding electrode. The electrogenic ion fluxes across the membrane were measured as a deflection from the baseline current. The whole setup was carefully grounded and shielded against external currents with a Faraday cage.

Currents were measured with Geneclamp 500 amplifier (Axon Instruments, Foster City, CA, USA) and recorded with a DIGIDATA 1322 A interface (Axon

Instruments, Foster City, CA, USA) on a computer for data storage and subsequent analysis using pClamp 9 (Axon Instruments, Foster City, CA, USA).

### 2.3.3.1 Pulse protocol

For the CIC-2 channel a holding potential of  $-60\text{mV}$  was used. Voltage steps of  $20\text{mV}$  from  $+40\text{mV}$  to  $-140\text{mV}$  for  $10\text{ sec}$  each followed by a depolarisation step by  $+50\text{mV}$  for  $3\text{ sec}$  were applied.

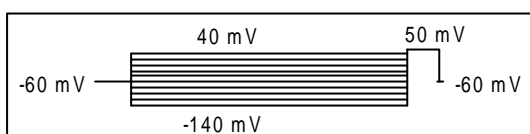


**Figure 9:** Pulse protocol. The individual voltage pulses are superimposed.

### 2.3.3.2 Experimental design

Voltage gated activation of CIC-2 channels was measured under isoosmotic conditions in ND96 superfusate. The Cell swelling induced activation of CIC-2 channels were measured in ND96 first and immediately afterwards in ND48 plus sucrose superfusate. Then sucrose was removed from the superfusate and oocytes were measured every five minutes in ND48 (hypoosmotic) superfusate.

## **2.3.4 Three dimensional structural model of the CBS1 domain of CIC-2**

The X-ray IMPDH dimer-CBS domains structure of the bacteria *S. pyrogens* (1zfi) were retrieved from the Protein Data Bank. Three dimensional structural model of the CBS1 domain of CIC-2 was modeled by Dr. Guiscard Seebohm (Department of Physiology, Tübingen). The construction was based on homology to IMPDH-CBS using the solved crystal structures of corresponding domains using a similar approach as reported by (Estevez *et al.*, 2004). The alignment of CIC-0 and mammalian homologues is shown in Figure 33. The CIC-2 models were generated using SWISS-MODEL (<http://www.expasy.org/swissmod/SWISS-MODEL.html>) and energy optimized using Gromos96 in default settings within the Swiss-PdbViewer (Guex & Peitsch, 1997). In the model with the lowest energy putative h-bonds with distances of 1.2 to 2.76 Angström were calculated. Subsequently, the virtual mutagenesis of Arg646 to Gln646 and energy optimized the resulting model using the same force field constraints were performed. In the R646Q-model with the lowest energy putative h-bonds with the same distances were calculated again.

## 3 Results

### 3.1 Molecular biology

#### 3.1.1 Frequency of polymorphisms

In the introns of the inhabitants of a malaria-endemic area in Lambaréné, Gabon, (see above) 10 mutations were found, none of which affected intron/exon boundaries. In the exons 11 mutations were found: 8 led to an amino acid exchange, 3 represent synonymous mutations. Most of the mutations were very low in frequency (under 0.1). The mutation I302I and S668T, however, were found in a frequency of 0.457 and 0.271, respectively (Table 2).

For this study the polymorphisms P48R, R68H, G199A, R646Q, R725W, and R747H (all of them found in the inhabitants of a malaria-endemic area but not in the Caucasian control group) were expressed in oocytes.

Table 2: Frequency of exon mutations in African individuals

Amino acid	Frequency of Wildtyp	Freq. of Mutant
P48R	0.986	0.011
R68H	0.942	0,058
I170I	0.986	0.011
G199A	0.986	0.011
I302I	0.543	0.457
N542N	0.986	0.011
R646Q	0.986	0.011
S661T	0.986	0.011

S668T	0.729	0.271
R725W	0.957	0.043
R747H	0.986	0.011

The sequence analysis from a Caucasian control group (see above) found neither the R646Q nor the S661T polymorphism in 191 blood samples. In contrast the frequency of these polymorphism were both 0.011 in the inhabitants of the malaria-endemic area in Lambaréné, Gabon (Table 3).

Table 3: Frequency of mutations in Caucasian and African individuals

Amino acid	Freq. in Caucasians	Freq. Africans
R646Q	0.000	0.011
S661T	0.000	0.011

### 3.1.2 Polymorphic positions in the Clcn2 gene

The DNA sequence of all 24 exons from 35 individuals was determined. A total of 12 fragments was amplified by PCR harboring all exons. DNA sequencing was done with the same primers used to generate the PCR products, or with primers internally to those (Tab. 1) . With the exons neighboring or intermediate intron sequences were analyzed as well. The coding region consists of 2694 bp. From adjacent intron sequences around 1500 base pairs were analyzed.

Table 4 shows the 25 flanking bases 3' and 5' of the Single Nucleotide Polymorphisms found in the exons and introns of the inhabitants of a malaria-endemic area in Lambaréné, Gabon. The numbering is according to accession nr NT\_005612.14; location in the intron and affected bases of the coding sequence are indicated.

**Table 4: Polymorphic positions in the CLCN2 gene**

2403	CGGATTTCGCCTGGGAGGGCCTGAAC (c/g) CTGGAAAGGTCCCCCTTCTCTCGG	P48R
2452	GAGCTCTTGGAATATGGACGGAGCC (g/a) TTGCGCCCGATGCCGCGGTGAGAAC	R68H
2555	AGCAGAGGCCATTAGAGCTGCTGAT (g/c) GGGGAGAGGGGACAGTTGAGGGGGC	INTRON
3285	CCCTCAGGCTGTCTGGTATGTTAGAA (g/a) AGAAGGGGAGGGCAGAGGCGGGACC	INTRON
3343	TGGGTGCATCGAATGCCTCTCCTGA (g/t) ACTGTTCCCTCTCCAGGCTCTGGCA	INTRON
3388	CTGGCATCCCTGAGATGAAGACCAT (c/t) TTGCGGGGAGTGGTGCTGAAAGAAT	I170I
3473	GGGCTGACCTGCGCCCTAGGCAGCG (g/c) GATGCCGCTTGGCAAAGAGGTA ACT	G199A
4196	TGCTGTTCTTCCCTTTAGAGACTAT (t/c) ACAGCCCTCTTCAAACCCGATTCC	I302I
6611	CCTTCCTCAGCCTCTGGCCACCCCC (c/g) CAGCCAACCCTCTGCCCAAGAGCGG	INTRON
6611	CCTTCCTCAGCCTCTGGCCACCCCC (cc/aa) AGCCAACCCTCTGCCCAAGAGCGGG	INTRON

6785	TCCACTGCCTCTTTCTCTTCCCACC (c/t) CCCTCCCTGAAGGAGCAGCATTGG	INTRON
7259	TCATGATCGCCGTCATCCTGGCCAA (c/t) GCTGTCGCCCAGAGTCTGCAGCCCT	N542N
8157	CAGAGCCACCCAGACCTCTCCACTA (t/a) CTGATCAGGAGGGTCCCCCTACCCC	S661T
8113	GCCCAGCTGAGCCCAGCCC GCCGGC (g/a) GCAGCACATGCAGGAGCGCAGAGCC	R646Q
8179	CTATCTGATCAGGAGGGTCCCCCTA (c/g) CCCTGAGGCTTCTGTCTGCTTCCAG	S668T
8224	CTTCCAGGTGAGGGGAAAAGCCACA (a/c) AACGCTTCCTAAATGTCATTGTGTA	INTRON
8674	CGCAGAGTCGGCAGGCATCGCCCTC (c/t) GGAGCCTCTTCTGTGGCAGTCCACC	R725W
8981	AAGAAGTTGGAATCCTGTGAGAAGC (g/a) CAAGCTGAAGCGTGTCCGAATCTCC	R747Q
8655	GTCCGAATCTCCCTGGCAGTAAGTA (t/g) GCCTGCTCTTCTAGCATCTCGGCGG	INTRON
9248	GCTGCTGTCCCATGGGAGGGACCA (c/a) GGGGTTGGAAAAAGGGCAGGCCAGC	INTRON
9306	GAGGTGAGGTGAGCTACAGGCACCT (t/g) TCTCCCTAACCTCATAGTCTCTTC	INTRON

## 3.2 Electrophysiology

Voltage-gated  $\text{Cl}^-$  currents generated by heterologously expressed CIC-2 variants as analyzed by two-electrode voltage-clamp.

### 3.2.1 Isoosmotic bath solution

To test for the functional significance of the identified polymorphisms in the *Clcn2* gene, wildtype and mutated CIC-2 mRNA (cRNA) was injected in *Xenopus laevis* oocytes and the CIC-2 channel activity determined by two-electrode voltage-clamp.

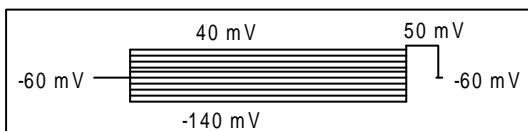


**Figure 10:** Applied pulse protocol which started at  $-60$  mV holding potential. Voltage steps of  $20$  mV from  $+40$  mV to  $-140$  mV were applied for  $10$  sec each followed by a depolarisation step to  $+50$  mV for  $3$  sec.

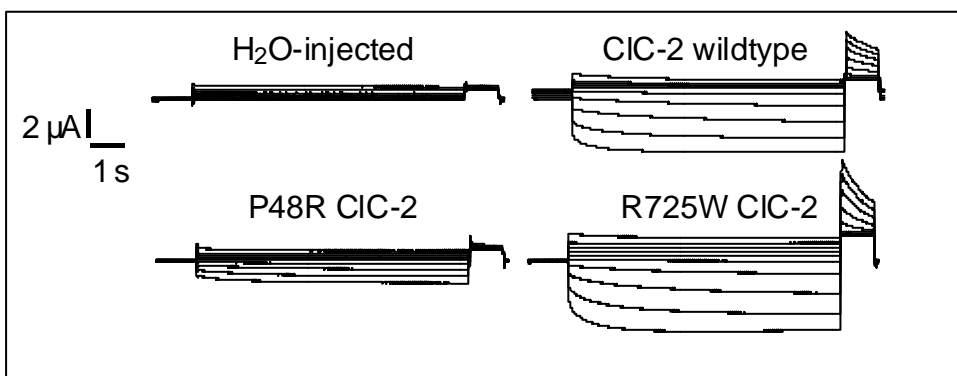


**Figure 11:** Current traces of a  $\text{H}_2\text{O}$ -injected oocyte (upper left), a CIC-2 wildtype mRNA (upper right) and two (P48R, R725W) CIC-2 mutant mRNA-injected oocytes (lower left and right). The currents were recorded  $2$  d after injection.

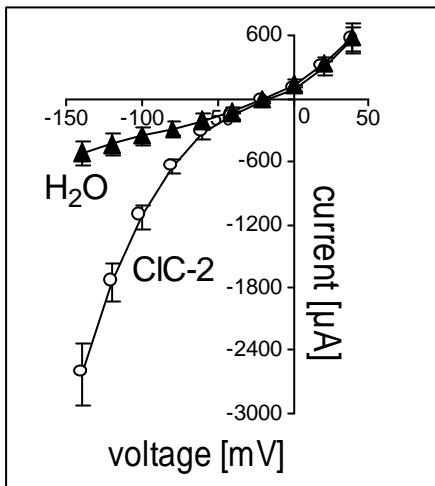


**Figure 12:** Current-voltage relationships of H<sub>2</sub>O-injected (closed triangles) and CIC-2 wildtype mRNA-injected oocytes (open circles) recorded 2d after injection (means  $\pm$  SE; n = 6-14). The steady state current at the end of the voltage sweep has been analyzed.

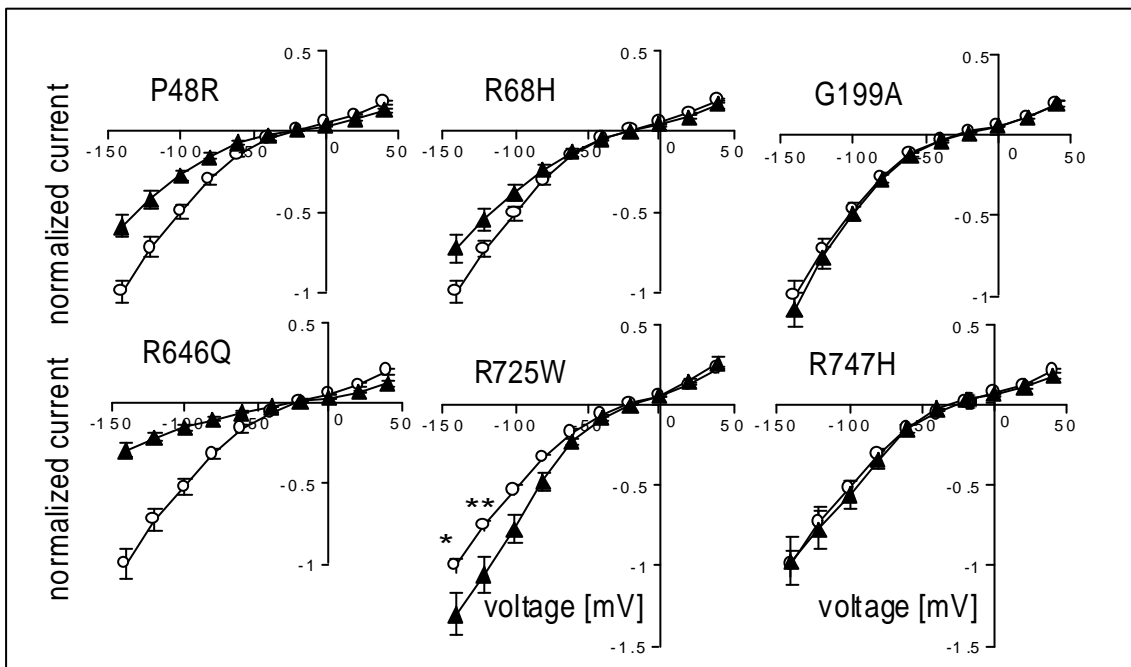


**Figure 13:** Normalized current-voltage relationships of wildtype mRNA-injected (open circles) and mutated CIC-2 mRNA-injected oocytes (closed triangles).

The amino acid exchange of the mutants is indicated. The currents of the mutants were determined in at least three different oocyte preparations. For each oocyte preparation wildtype mRNA was recorded in parallel (open circles) and currents were normalized to the -140 mV value of the corresponding wildtype CIC-2 current (means  $\pm$  SE; n = 12-72; \*, \*\*: p  $\leq$  0.05, 0.01; ANOVA).

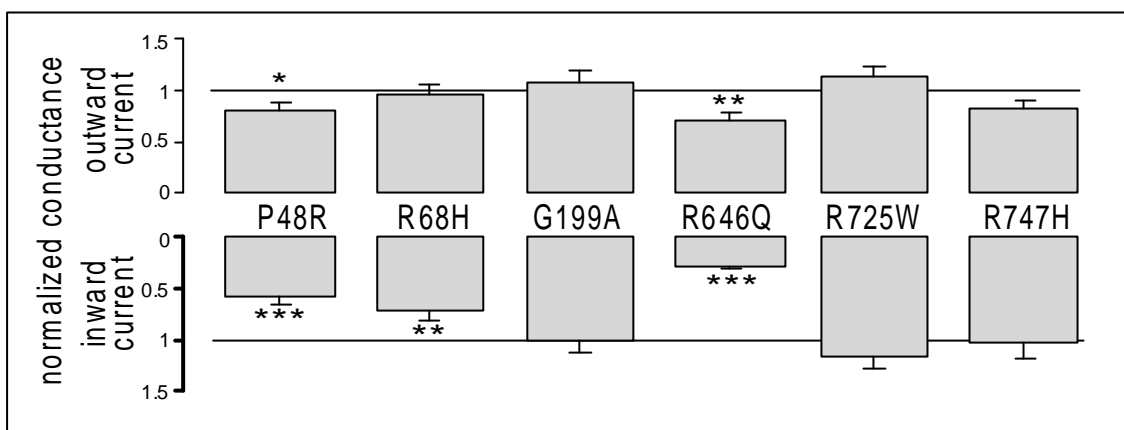


**Figure 14:** Normalized conductance as calculated from Fig. 13 for the outward and inward current by linear regression between 0 mV and 40 mV and -60 and -140 mV, respectively. Conductance were normalized to those of the wildtype CIC-2 (means  $\pm$  SE; n = 12-72; \*, \*\*, \*\*\*: p  $\leq$  0.05, 0.01, 0.001; two-tailed t-test).

### 3.2.1.1 Isotonic bath solution summary

Figure 12 shows the currents of water-injected and CIC-2 wildtype mRNA-infected oocytes as recorded in isotonic ND96 bath solution. Heterologously expressed CIC-2 exhibited an inwardly rectifying current-voltage relationship with a current reversal potential in the range of -20 to -30 mV (Figure 12). Two mutants (G199A and R747H) exhibited current-voltage relationships identical to the wildtype channel (Figure 13 and Figure 14). Three mutants (P48R, R68H, and R646Q) generated lower currents which resulted in a significant lower inward and (except R68H) also lower outward conductance as compared to the wildtype control (Figure 13 and Figure 14). The mutant R725W, in contrast, generated significant larger inward currents than wildtype CIC-2 at high negative voltages (Figure 13 and Figure 14).

## 3.2.2 Voltage dependence and kinetics (isoosmotic)

### 3.2.2.1 Activation kinetics (isoosmotic)

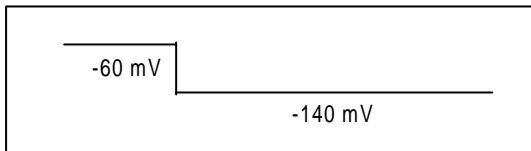


Figure 15: Pulse protocol of the analyzed part of the sweep. Slowly activating currents evoked by a voltage step from -60 mV holding potential to -140 mV voltage.

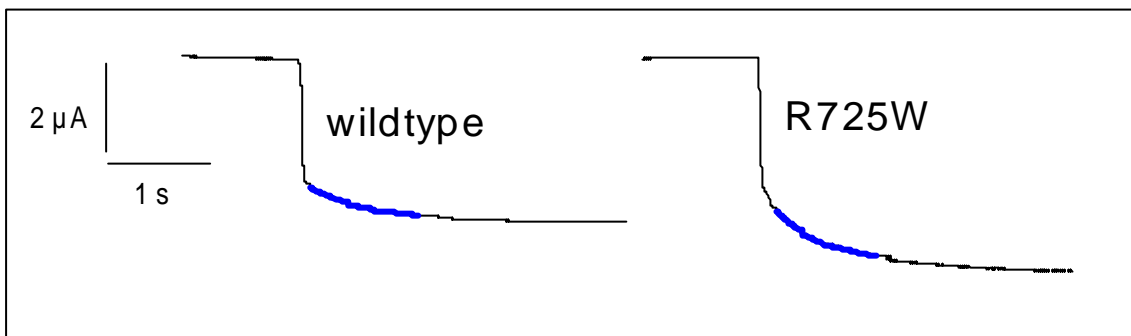


Figure 16: Current traces of a CIC-2 wildtype mRNA- (left) and a R725W-mutant mRNA-injected oocyte (right) are depicted. The hyperpolarization-stimulated time-dependently activating current was fitted mono-exponentially. The fitted curve is superimposed (bold line).

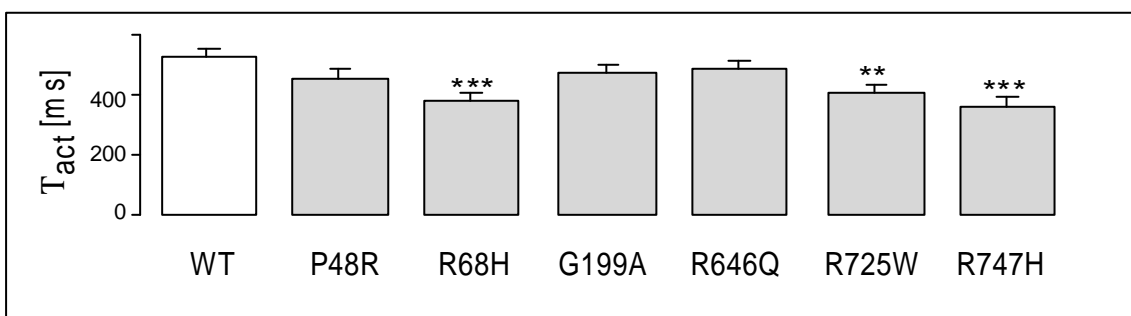
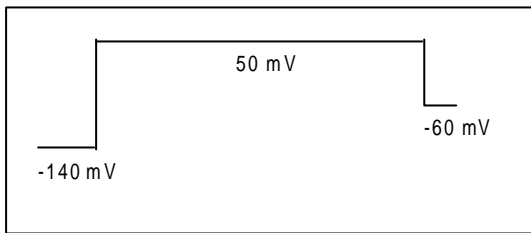
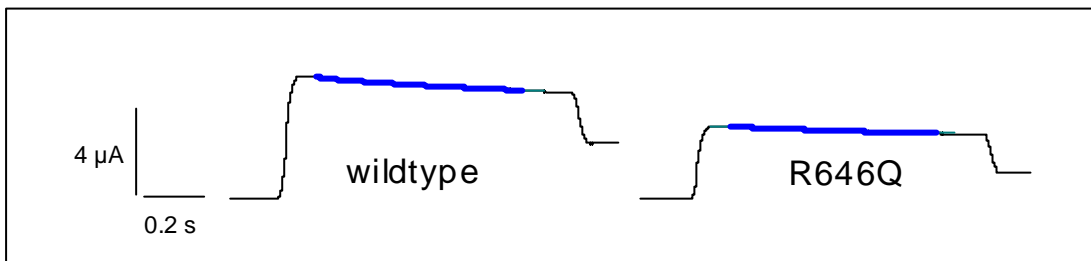


Figure 17: Mean time constant of activation ( $T_{act}$ ;  $\pm$  SE;  $n = 12-72$ ) determined as in Fig 16 of wildtype and mutant CIC-2 channels(\*, \*\*:  $p \leq 0.05, 0.01$ ; ANOVA).

### 3.2.2.2 Deactivation kinetics (isoosmotic)



**Figure 18:** Pulse protocol of analyzed part of the sweep for deactivating currents from -140 mV test potential to +50 mV voltage.



**Figure 19:** Deactivating currents of a wildtype mRNA- (left) and R646Q mutant CIC-2 mRNA-injected oocyte upon depolarization from -140 mV test potential to +50 mV voltage. Currents were fitted mono-exponentially. The fitted curve is superimposed (bold line).

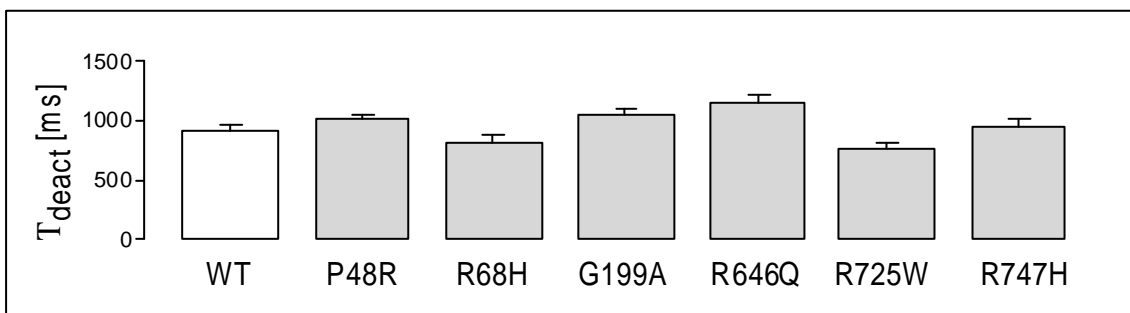


**Figure 20:** Mean time constant of de-activation ( $T_{deact}$ ;  $\pm$  SE;  $n = 12-72$ ) determined as in Fig 19 of wildtype and mutant CIC-2 channels (\*\*\*:  $p \leq 0.001$ ; ANOVA).

### 3.2.2.3 Half-maximal voltage

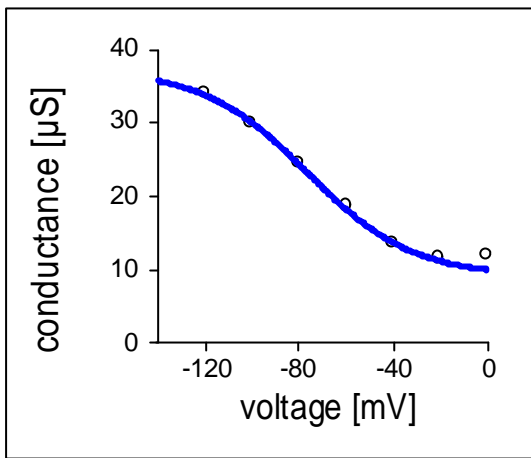


**Figure 21:** Dependence of wildtype CIC-2 channels on the voltage. The CIC-2-generated conductance was determined for the steady state current, plotted against the test potential and fitted by the Boltzmann equation (bold line).

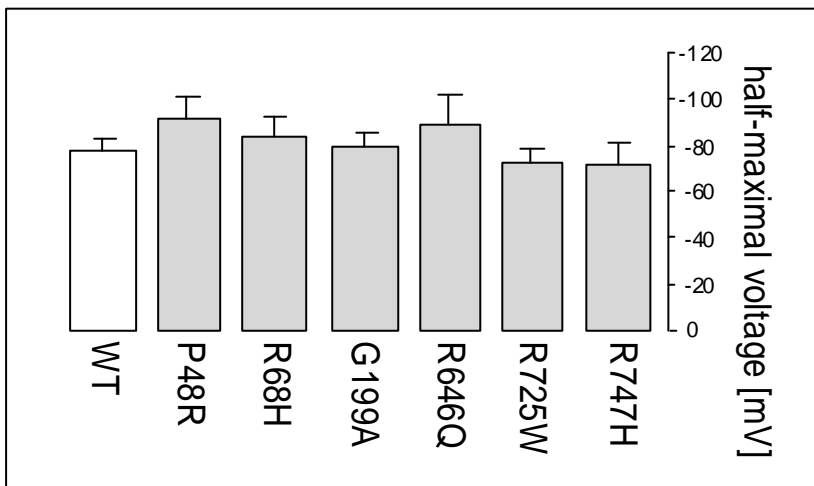


**Figure 22:** Mean half-maximal voltage ( $\pm$  SE;  $n = 11-73$ ) of wildtype and mutant CIC-2 channels as determined by a Boltzmann fit .

### **3.2.2.4 Summary of voltage dependence and kinetics of the CIC-2**

#### **channel variants**

Upon hyperpolarization from holding potential to -140 mV test voltage and repolarization from -140 mV to + 50 mV (Figure 16 and Figure 19) CIC-2 wildtype channels activated and deactivated with a time constant of about 0.5 s and 0.8 s, respectively (Figure 17 and Figure 20). P48R, G199A, and R646Q exhibited identical gating kinetics (Figure 17 and Figure 20). In contrast, the mutant R68H, R725W, and R747H channels showed significant faster activation (Figure 17) while deactivation was unaltered as compared to the wildtype channel (Figure 20). Hyperpolarization-stimulated activation occurred in wildtype CIC-2 and all mutant channels similarly with a half-maximal voltage of about -80 mV (Figure 21 and Figure 22).

In summary, all mutant channels except G199A differed either by absolute currents or by their gating kinetics from the wildtype channel.

### 3.2.3 Hypoosmotic cell swelling

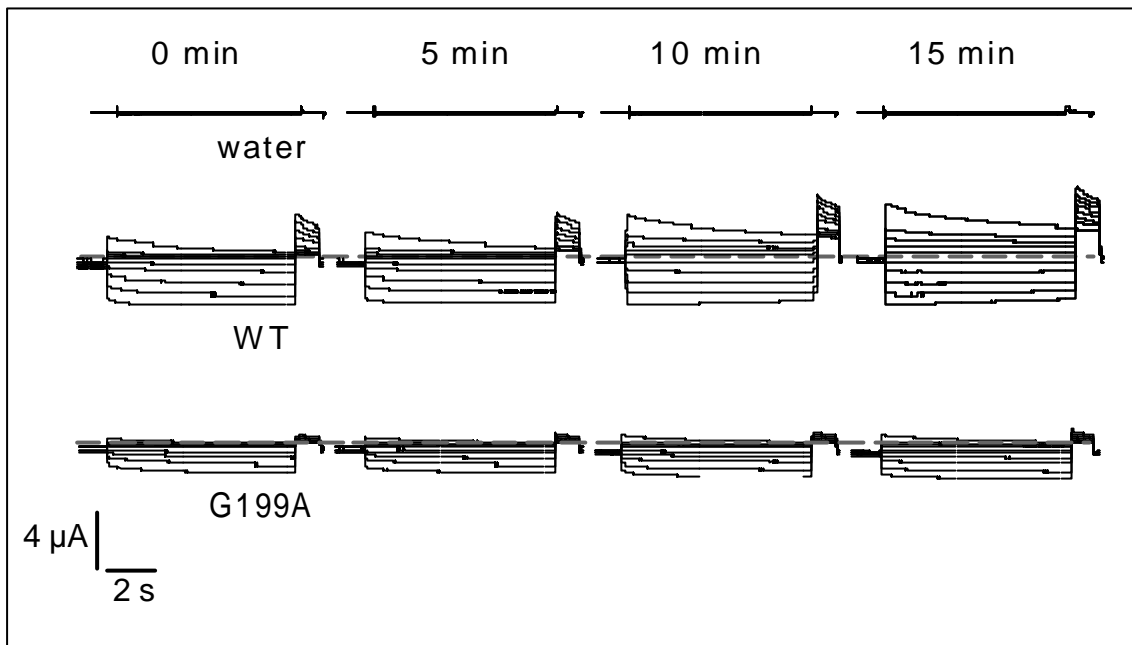


**Figure 23:** Current traces of a water-injected (upper traces), a CIC-2 wildtype mRNA-injected (middle traces), and a R199A mutant CIC-2 mRNA injected oocyte were recorded first in isotonic ND48+96 mM sucrose bath solution (0 min; left traces) and then after 5, 10 or 15 min (as indicated) of hypoosmotic swelling in ND48 bath solution (pulse protocol as in Fig. 10).

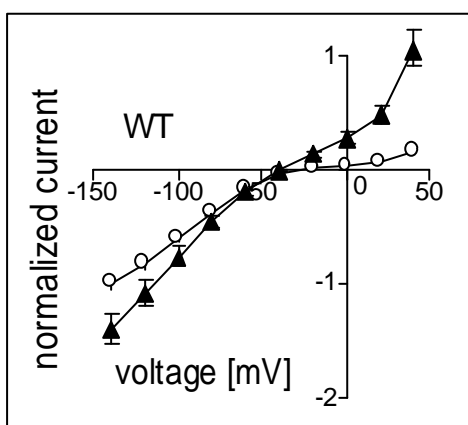


**Figure 24:** Mean current-voltage relationship ( $\pm$  SE;  $n = 10-17$ ) of CIC-2 wildtype mRNA-injected oocytes before (open circles) and during hypoosmotic swelling (15 min; closed triangles). Currents of each oocyte were normalized to the current

recorded under control conditions at -140 mV. The maximal currents of the voltage sweeps are depicted.

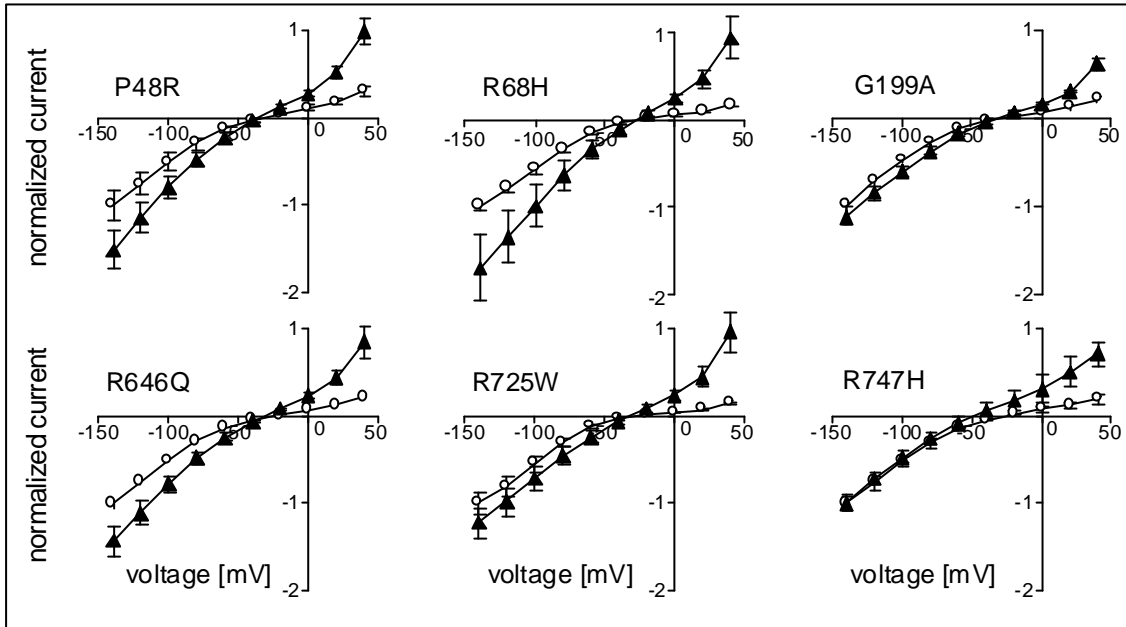


**Figure 25:** Mean current-voltage relationship ( $\pm$  SE;  $n = 7-13$ ) of hypotonically swollen (15 min) oocytes injected with different mutant CIC-2 mRNAs (closed triangles). The amino acid exchange of the mutants is indicated. For each oocyte preparation, swollen oocytes injected with wildtype mRNA were recorded in parallel (open circles). Currents were recorded as in Figure 24 and normalized to the -140 mV value of the corresponding wildtype CIC-2 current.

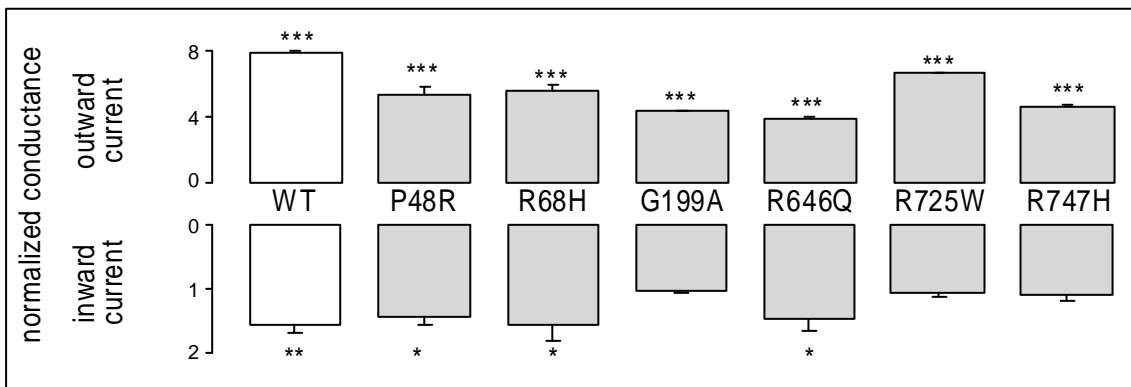


**Figure 26:** Mean conductance change ( $\pm$  SE;  $n = 7-13$ ) of wildtype- and mutant CIC-2 mRNA-injected oocytes evoked by hypotonic swelling (15 min).

Conductances before and during hypotonic swelling (15min) were calculated by linear regression between 0 and +40 mV and between -60 and -140 mV for the outward and inward currents, respectively. Conductance changes are determined by dividing the conductance of the hypotonically swollen cells by the initial conductance in isotonic bath solution.

### **3.2.3.1 Summary of hypoosmotic cell swelling-stimulated CIC-2 currents**

Hypotonic swelling of the oocytes by decreasing the bath osmolarity to 50% of ND96 solution stimulated an increase in wildtype CIC-2-generated inward and outward currents (Figure 23 and Figure 24). Similarly current increase was observed for P48R-, R68H-, and R646Q- mutant channels (Figure 25). Swelling, however, failed to stimulate the inward currents in G199A- R725W, and R747H- mutant CIC-2-injected oocytes, while the stimulated increase of outward currents generated by these three mutants was similar to that of the wildtype channel (Figure 25).

## 3.2.4 Voltage dependence and kinetics (hypoosmotic)

### 3.2.4.1 Activation kinetics (hypoosmotic)

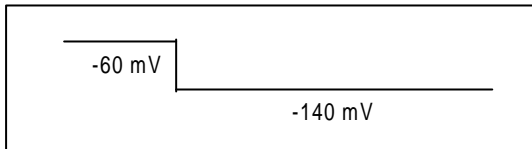


**Figure 27:** Pulse protocol of analyzed part of the sweep for activation. Slowly activating currents evoked by a voltage step from -60 mV holding potential to -140 mV voltage.

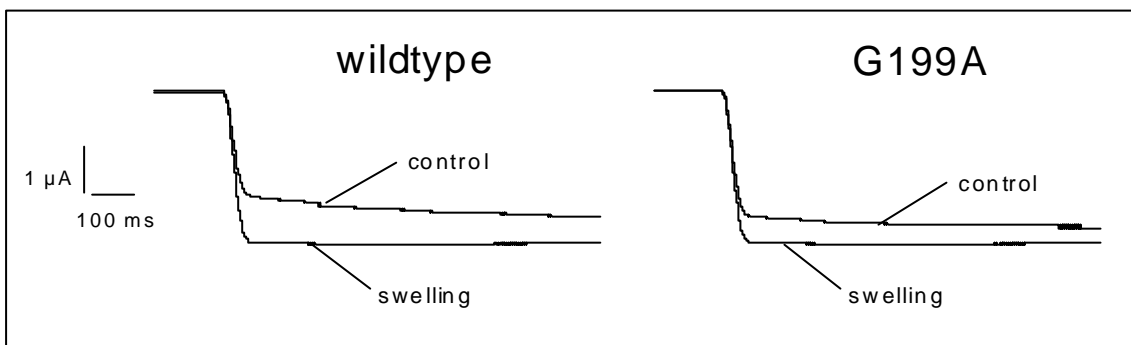


**Figure 28:** Slowly activating currents in non-swollen (ND48+98 mM sucrose; upper line) and swollen (15 min ND48, lower line) oocytes evoked by a voltage step from -60 mV holding potential to -140 mV voltage. Current traces of a ClC-2 wildtype mRNA- (left) and a G199A-mutant mRNA-injected oocyte (right) are shown. The hyperpolarization-stimulated time-dependently activating current was fitted mono-exponentially.

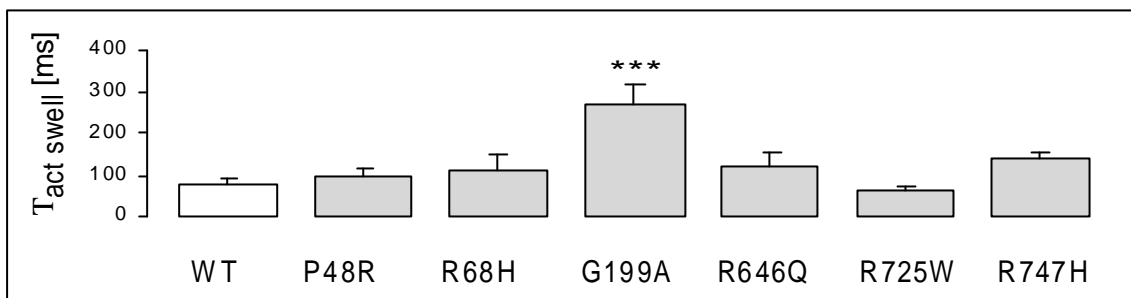


**Figure 29:** Mean time constant of activation (Tact-swell; + SE; n=6-10) determined as in Figure 28 during cell swelling) of wildtype and mutant CIC-2 channels (\*\*\*:  $p \leq 0.001$ ; ANOVA).

### 3.2.2.1 Deactivation kinetics (hypoosmotic)

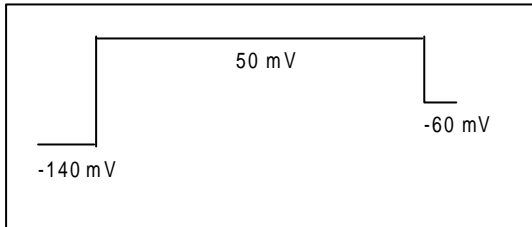


**Figure 30:** Pulse protocol of analyzed part of the sweep for deactivating currents from -140 mV test potential to +50 mV voltage.

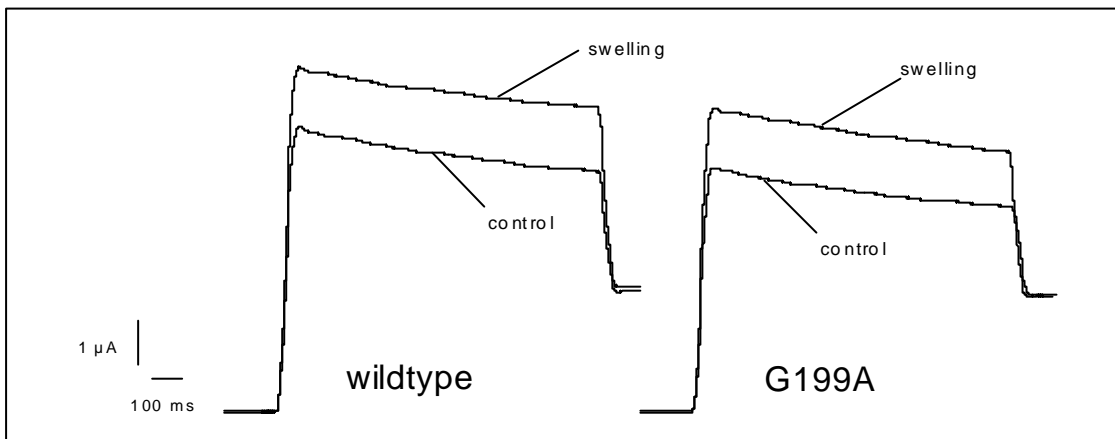


**Figure 31:** Deactivating currents in non-swollen (ND48+98 mM sucrose; lower line) and swollen (15 min ND48, upper line) oocytes of a wildtype mRNA- (left) and a G199A-mutant CIC-2 mRNA-injected oocyte (right) upon depolarization from -140 mV test potential to +50 mV voltage. Currents were fitted mono-exponentially.

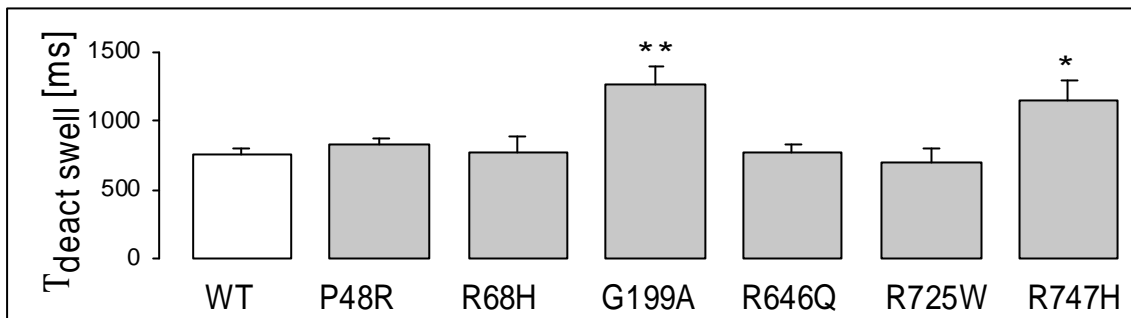


**Figure 32:** Mean time constant of de-activation ( $T_{\text{deact-swell}}$ ; + SE;  $n = 6-13$ ); determined as in Figure 31 during cell swelling of wildtype and mutant CIC-2 channels (\*, \*\*:  $p \leq 0.05, 0.01$ ; ANOVA).

### 3.2.4.1 CIC-2 activation and deactivation kinetics in hypotonically swollen cells summary

The swelling-stimulated current changes were accompanied by alterations of the gating kinetics.  $T_{\text{act}}$  decreased from about 0.5 s (Figure 17) to values below 100 ms (Figure 28 and Figure 29) in wildtype and most mutant CIC-2 channels. Remarkably, the G199A- and the R747H-mutant CIC-2 channels activated during cell swelling significantly (G199A) or in tendency (R747H) slower than wildtype CIC-2 (Figure 29). In addition to faster activation, cell swelling stimulated current inactivation at negative test potentials (Figure 27) and deactivation. The mean time constant of the latter ( $T_{\text{deact}}$ ) decreased during cell swelling from about 900 ms (Figure 20) towards 600 ms in wildtype and most mutant CIC-2 channels (Figure 31 and Figure 32). Again, G199A- and the R747H-mutant channels exhibited a significantly slower time constant of deactivation ( $T_{\text{act-swell}}$ ) than wildtype CIC-2 channels (Figure 32).

Taken together, the cell swelling experiments suggest an unaltered regulation by cell volume of P48R-, R68H-, and R646Q- mutant channels. R725W-mutant channels which show gating kinetics during cell swelling similar to that of the

wildtype channel exhibited no swelling-induced activation at hyperpolarizing voltages. Similarly, such swelling-stimulated increase in channel activity at hyperpolarizing voltages was also absent in G199A- and R747H-mutant channels. In sharp contrast to wildtype or R725W channels, cell-swelling did not accelerate the gating kinetics of these two mutants.

### 3.3 Model of CIC-2 channel

Figure 33 shows a structure model (see Figure 4) of a CIC-2 channel including the polymorphisms which were received from PD Dr. Kun (Department of Parasitology, University of Tübingen) for expression in oocytes (P48R, R68H, G199A, R646Q, R725W, and R747H). Those polymorphisms were identified in the human Clcn2 gene by sequence analysis in inhabitants of a malaria-endemic area in Lambaréné, Gabon (Africa).

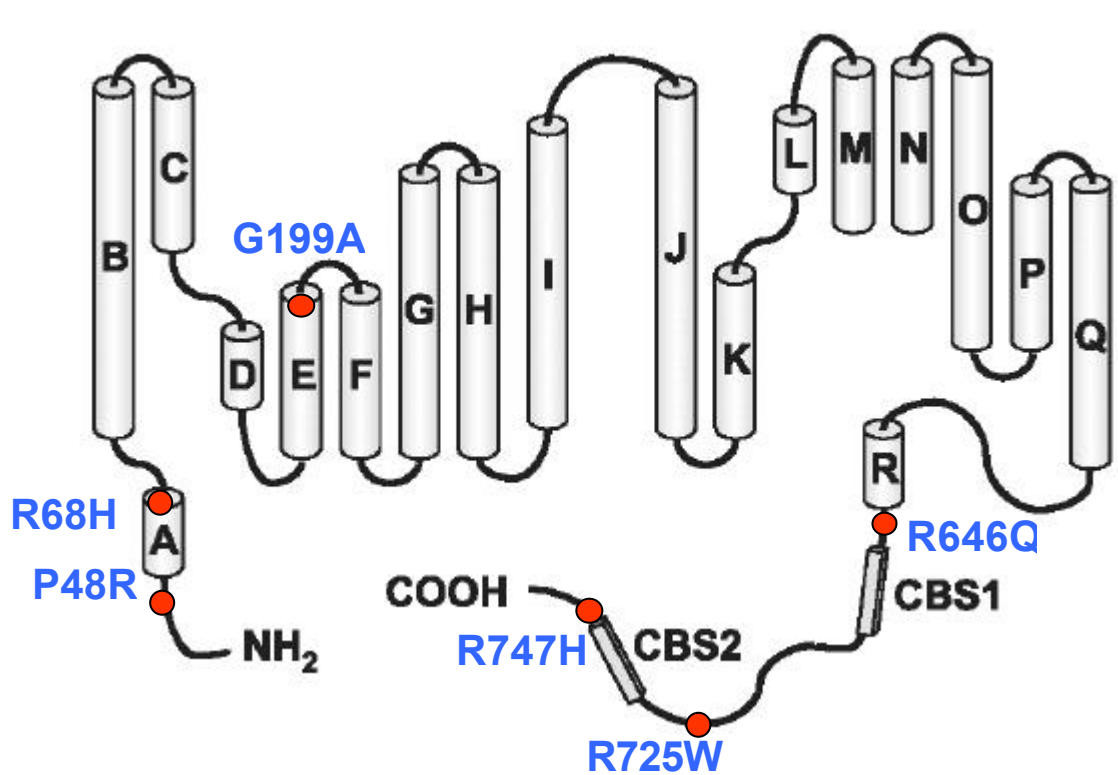


Figure 33: Model of CIC-2 channel including polymorphisms

## 3.4 Cystathionine Beta Synthase -1 domain

### 3.4.1 Alignment of the CBS-domains

			β-sheet	α-helix	β-sheet	β-sheet	α-helix
CBS1	IMPDH	StrPyo	DPFFLTPEHKVSEAEELMQR	YRIS	SGVPIVETLANRKL	VGII	TNRDMRFISDYNAPISEHMTSE
CBS1	IMPDH	HUMAN	DPVVLSPSHTVGDVLEAKMRHGF	SGIPITETGT	MGSKLVG	GIVTSRDIDFLAEKDHTLLSEVM	
CBS1	CLC1	HUMAN	DVKFVSASYTYGELR	TLLQTTT	VKTLPLVDSKDSM	ILLGSVERSELQALLQRHLC	PERRLRAA
CBS1	CLC2	HUMAN	DVPHVALSCTFRDLRLALHRTKGR	MALVESPESM	ILLGSIERSQV	VALLGAQLSPARRRQHM	
CBS1	CLC5	HUMAN	LTVLTQDSMTVEDVETII	SETTYS	GFPVVVSRESQ	RLVGFVLRRLDIISIENARKKQD	GVVST

**Figure 34:** CBS-domains of streptococcus, human IMPDH and human CLC channels

Figure 34 shows an alignment of the Cystathionine Beta Synthase-domains (CBS- domains) of streptococcus and human IMPDH and human CLC channels. This alignment was the basis of the generation of a 3D-model of CLC-CBS-domain1 and was generated on the basis of the crystal structure of IMPDH-CBS-domain from *Streptococcus pyrogens* (Figure 35). In the stereo-view representation the amino acids Val614, Val624 and Arg646 are shown in stick presentation. The respective residues form an h-bonding network in the model calculations.

### 3.4.2 CLC-CBS-domain1 3D-model

The general structural homology of two cystathionine beta-synthase-domains (CBS) in CLC-channels to a CBS-domain dimer of the bacterial inosine monophosphate dehydrogenase (IMPDH) (Zhang *et al.*, 1999) was shown by Estevez *et al.* (Estevez *et al.*, 2004). Dr. Guiscard Seebohm (Department of Physiology, Tübingen) modeled the first CBS-domain of CLC-2 and it is based on similarity to a dimer-CBS domain from IMPDH. A low-energy structural homology model is shown in Figure 35. This model suggests a hydrogen bond between the backbone of arginine646 with leucine614 connecting arginine646 with the anti-parallel beta -sheet of the CBS-domain possibly stabilizing the structure. Virtual mutagenesis of arginine646 to the here reported disease associated mutation R646Q mutation disrupts the hypothetical h-bond.

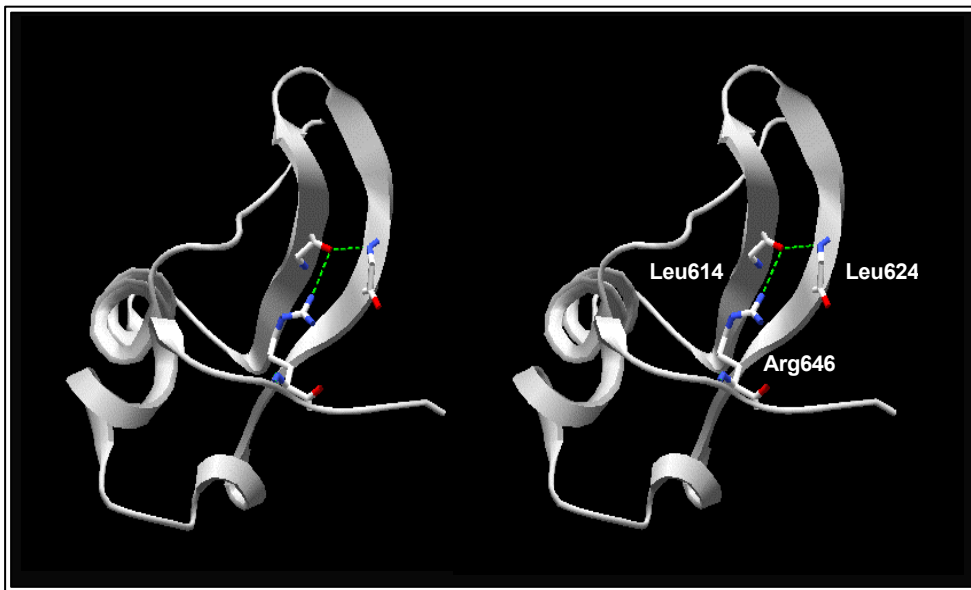


Figure 35: 3D-model of CLC-CBS-domain1

## **4 Discussion**

### **4.1 Sources of error**

#### **4.1.1 General aspects of the oocyte expression system**

*Xenopus laevis* oocytes are a popular tool for the functional expression of membrane proteins as described in the method section. Endogenous *Xenopus* proteins are possible sources of error because they might be similar to the ones that are thought to be studied. Endogenous *Xenopus* proteins could be activated by substances injected into the oocyte. Furthermore, intracellular signalling pathways examined in oocytes do not necessarily correspond to mammalian cell pathways. Different proteins from the native cell that are missing in the oocyte could alter the function of the protein expressed. However, *Xenopus* oocytes allow a clear cut between a real transport process and an artefact: the relatively high amounts of injected cRNA lead to an extremely high expression of the protein to be studied. In each experiment the cRNA injected oocytes are compared to water injected oocytes to exclude that an endogenous transporter is being studied.

#### **4.1.2 Oocytes and cRNA**

The quality of Oocytes and cRNA have an enormous influence on the expression rate observed under experimental conditions. The resulting variation depends on the frog prepared, the age of the oocyte and the collagenase used for the preparation. Similarly, there are differences in the results depending on the quality of the cRNA. It is important that the cRNA contains no residues from unincorporated nucleotides or the reagents it has been cleaned with such as ethanol or lithium with regards to its purity. Fresh preparations at every second month and storage at - 80°C and help preventing a degradation of the cRNA. 5 – 10 oocytes were checked prior to each experiment for their protein expression in order to minimize the variables mentioned above. In addition, a series of

experiments was not carried out on a single oocyte preparation but repeated instead with oocytes from different frogs.

### **4.1.3 Solutions**

The osmolarity and the pH of the solutions used (as mentioned above) were checked on a daily basis. Deviations more than 1% were not tolerated. All the solutions were kept at 4°C until the experiment. All the chemicals were kept at the temperature recommended by the vendor and all chemicals protected from light.

## 4.2 Identification of polymorphisms

The present study identified variations of the *Clcn2* gene in an African population. These variations comprise modification of the N-terminus (P48R, R68H), of a putative extracellular loop (G199A), and of the C-terminus (R646Q, S661T, R725W, R747H).

The frequency of the two polymorphisms R646Q and S661T were both 0.011 in the inhabitants of the malaria-endemic area in Lambaréné, Gabon. In contrast, none of these two polymorphisms was found in a Caucasian control group. This might be due to the bottleneck phenomenon. Due to the migration of only a small part of the African population to Europe the gene pool present in Europe is much smaller than in Africa.

### 4.3 Functional characterization of polymorphisms

Regulation of CIC-2 by membrane voltage, cell swelling and pH has been demonstrated to be linked to the cytosolic N-terminus of the channel protein (Grunder *et al.*, 1992; Jordt & Jentsch, 1997). 15 amino acids of the N-terminus form an essential domain that inactivates the channel under resting condition by binding to an internal receptor of the channel protein. Further N-terminal amino acids contribute to this inactivation (Grunder *et al.*, 1992). In the present study the mutant P48R channel generated less steady state current than wildtype CIC-2. P48R is C-terminal from the essential inactivation domain (Grunder *et al.*, 1992). Since P48R and wildtype CIC-2 exhibited similar swelling- and hyperpolarization-induced activation and gating kinetics, a function of P48R in the inactivation complex is not probable. Rather a lower surface expression of P48R than wildtype CIC-2 might be suggested implying an interaction of this NH<sub>2</sub>-terminal site with proteins that regulate cycling of CIC-2 into or from the plasma membrane or that stabilize the channels in the membrane. An interaction of the CIC-2 N-terminus with the cytoskeleton has been proposed (Ahmed *et al.*, 2000).

A further mutation in the N-terminus, R68H, resulted in both, decrease of steady state current and faster activation of the CIC-2 channels. The altered activation kinetics was apparent under isosmotic recording condition but disappeared during hypotonic swelling. This might suggest that R68 contributes to the N terminal inactivation complex.

The loop between the alpha helices E and F in the CIC-2 protein contributes to the selectivity filter of the channel (Dutzler *et al.*, 2002). The G199A mutation identified in the present study resides in this loop and is N-terminal from the selective filter-forming amino acids. G199A did not affect current or gating kinetics when records were obtained under isosmotic conditions. In contrast to wildtype CIC-2, hypotonic swelling, however, did not accelerate the

hyperpolarization-stimulated gating of G199A at negative voltage and, thus, did not increase steady state inward current suggesting that G199A contributes to swelling-induced channel activation.

Three further mutations, R646Q, R725W, and R747H were located in the cytosolic C-terminus N-terminal of CBS domain 1, between CBS domain 1 and 2, and C-terminal of CBS domain 2, respectively. CBS domains (named after Cystathionine Beta Synthase) (Bateman, 1997) bind adenosyl residues of molecules such as ATP or AMP. The CBS domains of CIC-2 have been demonstrated to similarly bind ATP (Abu-Hamdah *et al.*, 2004). Replacement of ATP by AMP reportedly accelerates the opening and closing kinetics of CIC-2 channels (Niemeyer *et al.*, 2004). Mutations in this region such as G715E (Haug *et al.*, 2003) alter the effect of nucleotides on the channel (Niemeyer *et al.*, 2004). Moreover, truncation of CBS-2 probably disrupts CLC channel function as demonstrated for CIC-1 (Hebeisen *et al.*, 2004). The mutation R725W of the present study activated faster during hyperpolarization and generated larger steady state currents than the wildtype channel when recorded under isosmotic conditions. Similarly, the mutation R747H showed faster activation during hyperpolarization but identical steady state currents as compared to wildtype CIC-2. Hypotonic cell swelling did not activate inward currents of R725W or R747H mutant channels. Taken together, these data indicate modulation of the hyperpolarization- or swelling-induced channel gating by mutations in the C-terminus. A third C-terminal mutation R646Q resulted in a strong decrease of the heterologously expressed current as compared to that of the wildtype channel. The R646Q-generated current did, however, not differ in gating kinetics or swelling-induced activation from the wildtype current suggesting reduced surface expression of R646Q. Modelling of the first CBS-domain of CIC-2 suggested a hydrogen bond of R646 with L614. Virtual mutagenesis hints to a disruption of this hydrogen bond in the R646Q mutant which might destabilize the CBS domain. However, the similarity of CIC-2 with the template inosine monophosphate dehydrogenase from *Streptococcus pyogenes* (Zhang *et al.*, 1999) is relatively low. Nevertheless, the data might

hint to a role of CBS-1 and R646 in the surface expression of the channel even though deletion of CBS-1 in CIC-1 channels have been demonstrated to be tolerated (Hebeisen *et al.*, 2004).

## **4.4 Influence of polymorphisms on malaria**

Since the frequency of the functional mutations is very low an influence of these mutations on the course of malaria can not be deduced. Although accumulation of low frequent mutations in one gene can lead to susceptibility or resistance of complex diseases (Smirnova *et al.*, 2003) we do not find statistically significant trends. Neither the frequency of single nor combined mutations (either functional or non-functional) was distributed unequally in the case-control study. Most of the changes occur in the intracellular domains of the molecule; also the only coding SNP between chimpanzee and human occurs here (at residue 730). Obviously functional constraints are more relaxed in these domains than in the rest of the molecule that form the pore. Changes in the amino acid sequence are tolerated because selection may improve interaction to intracellular proteins, which in consequence leads to an altered activity of the channel. Faster opening or longer opening periods of the channel may introduce subtle changes in the physiology of the cell important for selection processes such as defense against intracellular microbes other than malaria parasites.

## 5 Summary

The human malaria parasite *Plasmodium falciparum* has been demonstrated to activate CIC-2 Cl<sup>-</sup> channels of the host erythrocyte during its endoerythrocytic stage of life cycle. This activation contributes to the host cell volume homeostasis. Six amino acid exchanges (P48R, R68H, G199A, R646Q, R725W, and R747H) were identified in low frequency in the CIC-2-encoding *Clcn2* gene in a population living in a malaria-endemic area (Gabon) but not in a Caucasian control group.

Cl<sup>-</sup> currents were determined by two-electrode voltage-clamp in heterologous expression of CIC-2 channels carrying these polymorphisms in *Xenopus laevis* oocytes. Polymorphisms were measured under isoosmotic and hypoosmotic conditions. Activation and deactivation kinetics were determined. The three-dimensional crystal structure revealed that the Cl<sup>-</sup> channels are homodimers and each sub-unit within the dimer forms its own ion-conducting pore. Both of the sub-units interact at a broad interface. In addition it consists of two Cystathionine Beta Synthase domains (CBS-domains) located at the C-terminus. The CBS domains of CIC-2 bind ATP and influence the opening and closing kinetics of CIC-2 channels.

The polymorphisms investigated in this study comprise modification of the intracellular N-terminus (P48R, R68H), of a putative extracellular loop (G199A) and of the intracellular C-terminus (R646Q, R725W, R747H). This study suggests that one polymorphism (P48R) had a lower surface expression than wildtype CIC-2. This might be due to an interaction of this NH<sub>2</sub>-terminal site with proteins that regulate cycling of CIC-2 into or from the plasma membrane or that stabilize the channels in the membrane. Polymorphism R68H might contribute to the N-terminal inactivation complex. A mutation located at a putative extracellular loop (G199A) might influence swelling-induced channel activation. Mutations in the C-terminus (R725W and R747H) probably results in the modulation of the hyperpolarization- or swelling-induced channel gating.

Furthermore, the data might hint to a role of CBS-1 and therefore R646Q (which is located very close to CBS 1) in the surface expression of the channel.

In conclusion, these Clcn2 polymorphisms do result in altered ClC-2 channel functions. Since the frequency of the functional mutations is very low an influence of these mutations on the course of malaria can not be deduced. Alterations in the the blood stage of the malaria infection or the aetiopathology in combination with the polymorphisms could not be made.

## 6 References

- ABU-HAMDAH, R., CHO, W. J., CHO, S. J., JEREMIC, A., KELLY, M., ILIE, A. E. & JENA, B. P. (2004). Regulation of the water channel aquaporin-1: isolation and reconstitution of the regulatory complex. *Cell Biol Int* **28**, 7-17.
- AHMED, N., RAMJEESINGH, M., WONG, S., VARGA, A., GARAMI, E. & BEAR, C. E. (2000). Chloride channel activity of ClC-2 is modified by the actin cytoskeleton. *Biochem J* **352 Pt 3**, 789-794.
- BATEMAN, A. (1997). The structure of a domain common to archaebacteria and the homocystinuria disease protein. *Trends Biochem Sci* **22**, 12-13.
- BECK, J. S. & SAARI, J. T. (1977). Permeability coefficients by the hemolytic method: a correction. *Biophys J* **17**, 281-282.
- BOSL, M. R., STEIN, V., HUBNER, C., ZDEBIK, A. A., JORDT, S. E., MUKHOPADHYAY, A. K., DAVIDOFF, M. S., HOLSTEIN, A. F. & JENTSCH, T. J. (2001). Male germ cells and photoreceptors, both dependent on close cell-cell interactions, degenerate upon ClC-2 Cl(-) channel disruption. *Embo J* **20**, 1289-1299.
- CAREW, M. A. & THORN, P. (1996). Identification of ClC-2-like chloride currents in pig pancreatic acinar cells. *Pflugers Arch* **433**, 84-90.
- CHESNOY-MARCAIS, D. & FRITSCH, J. (1994). Activation of hyperpolarization and atypical osmosensitivity of a Cl<sup>-</sup> current in rat osteoblastic cells. *J Membr Biol* **140**, 173-188.
- CID, L. P., MONTROSE-RAFIZADEH, C., SMITH, D. I., GUGGINO, W. B. & CUTTING, G. R. (1995). Cloning of a putative human voltage-gated chloride channel (ClC-2) cDNA widely expressed in human tissues. *Hum Mol Genet* **4**, 407-413.
- CLARK, S., JORDT, S. E., JENTSCH, T. J. & MATHIE, A. (1998). Characterization of the hyperpolarization-activated chloride current in dissociated rat sympathetic neurons. *J Physiol* **506**, 665-678.
- DESAI, S. A., BEZRUKOV, S. M. & ZIMMERBERG, J. (2000). A voltage-dependent channel involved in nutrient uptake by red blood cells infected with the malaria parasite. *Nature* **406**, 1001-1005.
- DUMONT, J. N. (1972). Oogenesis in *Xenopus laevis* (Daudin). I. Stages of oocyte development in laboratory maintained animals. *J Morphol* **136**, 153-179.

- DURANTON, C., HUBER, S., TANNEUR, V., LANG, K., BRAND, V., SANDU, C. & LANG, F. (2003). Electrophysiological properties of the Plasmodium Falciparum-induced cation conductance of human erythrocytes. *Cell Physiol Biochem* **13**, 189-198.
- DURANTON, C., HUBER, S. M., TANNEUR, V., BRAND, V. B., AKKAYA, C., SHUMLINA, E. V., SANDU, C. D. & LANG, F. (2004). Organic Osmolyte Permeabilities of the Malaria-induced Anion Conductances in Human Erythrocytes. *J Gen Physiol* **123**, 417-426.
- DUTZLER, R., CAMPBELL, E. B., CADENE, M., CHAIT, B. T. & MACKINNON, R. (2002). X-ray structure of a ClC chloride channel at 3.0 Å reveals the molecular basis of anion selectivity. *Nature* **415**, 287-294.
- EGEE, S., HARVEY, B. J. & THOMAS, S. (1997). Volume-activated DIDS-sensitive whole-cell chloride currents in trout red blood cells. *J Physiol* **504**, 57-63.
- EGEE, S., LAPAIX, F., COSSINS, A. R. & THOMAS, S. L. (2000). The role of anion and cation channels in volume regulatory responses in trout red blood cells. *Bioelectrochemistry* **52**, 133-149.
- EGEE, S., LAPAIX, F., DECHERF, G., STAINES, H. M., ELLORY, J. C., C., D. & THOMAS, S. L. Y. (2002). A stretch-activated anion channel is up-regulated by the malaria parasite *Plasmodium falciparum*. *J. Physiol.* **542**, 795-801.
- EGEE, S., MIGNEN, O., HARVEY, B. J. & THOMAS, S. (1998). Chloride and non-selective cation channels in unstimulated trout red blood cells. *J Physiol* **511 ( Pt 1)**, 213-224.
- ELLORY, J. C. & HALL, A. C. (1988). Human red cell volume regulation in hypotonic media. *Comp Biochem Physiol A* **90**, 533-537.
- ESTEVEZ, R., PUSCH, M., FERRER-COSTA, C., OROZCO, M. & JENTSCH, T. J. (2004). Functional and structural conservation of CBS domains from CLC chloride channels. *J Physiol* **557**, 363-378.
- FRITSCH, J. & EDELMAN, A. (1996). Modulation of the hyperpolarization-activated Cl<sup>-</sup> current in human intestinal T84 epithelial cells by phosphorylation. *J Physiol* **490 ( Pt 1)**, 115-128.
- FURUKAWA, T., OGURA, T., KATAYAMA, Y. & HIRAOKA, M. (1998). Characteristics of rabbit ClC-2 current expressed in *Xenopus* oocytes and its contribution to volume regulation. *Am J Physiol* **274**, C500-512.
- GINSBURG, H. & KIRK, K. (1998). Membrane transport in malaria-infected erythrocyte. In *Malaria : Parasite biology, pathogenesis and protection*. ed. MICROBIOLOGY, A. S. F., pp. 219-232. Sherman IW, Wahington DC.

- GINSBURG, H. & STEIN, W. D. (2004). The new permeability pathways induced by the malaria parasite in the membrane of the infected erythrocyte: comparison of results using different experimental techniques. *J Membr Biol* **197**, 113-134.
- GRUNDER, S., THIEMANN, A., PUSCH, M. & JENTSCH, T. J. (1992). Regions involved in the opening of CIC-2 chloride channel by voltage and cell volume. *Nature* **360**, 759-762.
- GUEX, N. & PEITSCH, M. C. (1997). SWISS-MODEL and the Swiss-PdbViewer: an environment for comparative protein modeling. *Electrophoresis* **18**, 2714-2723.
- GYOMOREY, K., YEGER, H., ACKERLEY, C., GARAMI, E. & BEAR, C. E. (2000). Expression of the chloride channel CIC-2 in the murine small intestine epithelium. *Am J Physiol Cell Physiol* **279**, C1787-1794.
- HAMILL, O. P. (1983). Potassium and chloride channels in red blood cells. In *Single Channel Recording*. ed. NEHER, E., pp. 451–471. Plenum, New York.
- HAUG, K., WARNSTEDT, M., ALEKOV, A. K., SANDER, T., RAMIREZ, A., POSER, B., MALJEVIC, S., HEBEISEN, S., KUBISCH, C., REBSTOCK, J., HORVATH, S., HALLMANN, K., DULLINGER, J. S., RAU, B., HAVERKAMP, F., BEYENBURG, S., SCHULZ, H., JANZ, D., GIESE, B., MULLER-NEWEN, G., PROPPING, P., ELGER, C. E., FAHLKE, C., LERCHE, H. & HEILS, A. (2003). Mutations in CLCN2 encoding a voltage-gated chloride channel are associated with idiopathic generalized epilepsies. *Nat Genet* **33**, 527-532.
- HEBEISEN, S., BIELA, A., GIESE, B., MULLER-NEWEN, G., HIDALGO, P. & FAHLKE, C. (2004). The role of the carboxyl terminus in CIC chloride channel function. *J Biol Chem* **279**, 13140-13147.
- HOF, H., MÜLLER, R., L. & DÖRRIES, R. (2000). *Mikrobiologie*. Thieme, Stuttgart.
- HUBER, S. M., DURANTON, C., HENKE, G., VAN DE SAND, C., HEUSSLER, V., SHUMILINA, E., SANDU, C. D., TANNEUR, V., BRAND, V., KASINATHAN, R. S., LANG, K. S., KREMSNER, P. G., HUBNER, C. A., RUST, M. B., DEDEK, K., JENTSCH, T. J. & LANG, F. (2004). Plasmodium induces swelling-activated CIC-2 anion channels in the host erythrocyte. *J Biol Chem* **279**, 41444-41452.
- HUBER, S. M., GAMPER, N. & LANG, F. (2001). Chloride conductance and volume-regulatory nonselective cation conductance in human red blood cell ghosts. *Pflugers Arch* **441**, 551-558.

- HUBER, S. M. & HORSTER, M. F. (1996). Ontogeny of apical membrane ion conductances and channel expression in cortical collecting duct cells. *Am J Physiol* **271**, F698-708.
- HUBER, S. M. & HORSTER, M. F. (1998). Expression of a hypotonic swelling-activated Cl conductance during ontogeny of collecting duct epithelium. *Am J Physiol* **275**, F25-32.
- HUBER, S. M., UHLEMANN, A. C., GAMPER, N. L., DURANTON, C., KREMSNER, P. G. & LANG, F. (2002). Plasmodium falciparum activates endogenous Cl(-) channels of human erythrocytes by membrane oxidation. *Embo J* **21**, 22-30.
- JENTSCH, T. J., FRIEDRICH, T., SCHRIEVER, A. & YAMADA, H. (1999). The CLC chloride channel family. *Pflugers Arch* **437**, 783-795.
- JENTSCH, T. J., GUNTHER, W., PUSCH, M. & SCHWAPPACH, B. (1995). Properties of voltage-gated chloride channels of the CLC gene family. *J Physiol* **482**, 19S-25S.
- JENTSCH, T. J., STEIN, V., WEINREICH, F. & ZDEBIK, A. A. (2002). Molecular structure and physiological function of chloride channels. *Physiol Rev* **82**, 503-568.
- JORDT, S. E. & JENTSCH, T. J. (1997). Molecular dissection of gating in the CLC-2 chloride channel. *Embo J* **16**, 1582-1592.
- KAJITA, H., OMORI, K. & MATSUDA, H. (2000). The chloride channel CLC-2 contributes to the inwardly rectifying Cl- conductance in cultured porcine choroid plexus epithelial cells. *J Physiol* **523 Pt 2**, 313-324.
- KIRK, K. (2001). Membrane transport in the malaria-infected erythrocyte. *Physiol Rev* **81**, 495-537.
- KIRK, K. (2004). Channels and transporters as drug targets in the Plasmodium-infected erythrocyte. *Acta Trop* **89**, 285-298.
- KIRK, K., ASHWORTH, K. J., ELFORD, B. C., PINCHES, R. A. & ELLORY, J. C. (1991). Characteristics of <sup>86</sup>Rb<sup>+</sup> transport in human erythrocytes infected with Plasmodium falciparum. *Biochim Biophys Acta* **1061**, 305-308.
- KIRK, K. & HORNER, H. A. (1995). In search of a selective inhibitor of the induced transport of small solutes in Plasmodium falciparum-infected erythrocytes: effects of arylaminobenzoates. *Biochem J* **311**, 761-768.
- KIRK, K., HORNER, H. A., ELFORD, B. C., ELLORY, J. C. & NEWBOLD, C. I. (1994). Transport of diverse substrates into malaria-infected erythrocytes via a

pathway showing functional characteristics of a chloride channel. *J Biol Chem* **269**, 3339-3347.

KIRK, K., HORNER, H. A., SPILLETT, D. J. & ELFORD, B. C. (1993). Glibenclamide and meglitinide block the transport of low molecular weight solutes into malaria-infected erythrocytes. *FEBS Lett* **323**, 123-128.

KOMWATANA, P., DINUDOM, A., YOUNG, J. A. & COOK, D. I. (1994). Characterization of the Cl<sup>-</sup> conductance in the granular duct cells of mouse mandibular glands. *Pflugers Arch* **428**, 641-647.

KRUGLIAK, M., ZHANG, J. & GINSBURG, H. (2002). Intraerythrocytic Plasmodium falciparum utilizes only a fraction of the amino acids derived from the digestion of host cell cytosol for the biosynthesis of its proteins. *Mol Biochem Parasitol* **119**, 249-256.

KUN, J. F., LEHMAN, L. G., LELL, B., SCHMIDT-OTT, R. & KREMSNER, P. G. (1999). Low-dose treatment with sulfadoxine-pyrimethamine combinations selects for drug-resistant Plasmodium falciparum strains. *Antimicrob Agents Chemother* **43**, 2205-2208.

KUN, J. F., MORDMULLER, B., LELL, B., LEHMAN, L. G., LUCKNER, D. & KREMSNER, P. G. (1998). Polymorphism in promoter region of inducible nitric oxide synthase gene and protection against malaria. *Lancet* **351**, 265-266.

KUTNER, S., BREUER, W. V., GINSBURG, H. & CABANTCHIK, Z. I. (1987). On the mode of action of phlorizin as an antimalarial agent in in vitro cultures of Plasmodium falciparum. *Biochem Pharmacol* **36**, 123-129.

LEW, V. L. & HOCKADAY, A. R. (1999). The effects of transport perturbations on the homeostasis of erythrocytes. *Novartis Found Symp* **226**, 37-50.

LEW, V. L., MACDONALD, L., GINSBURG, H., KRUGLIAK, M. & TIFFERT, T. (2004). Excess haemoglobin digestion by malaria parasites: a strategy to prevent premature host cell lysis. *Blood Cells Mol Dis* **32**, 353-359.

LEW, V. L., TIFFERT, T. & GINSBURG, H. (2003). Excess hemoglobin digestion and the osmotic stability of Plasmodium falciparum-infected red blood cells. *Blood* **101**, 4189-4194.

MILLER, G. W. & SCHNELLMANN, R. G. (1994). A putative cytoprotective receptor in the kidney: relation to the neuronal strychnine-sensitive glycine receptor. *Life Sci* **55**, 27-34.

MURRAY, C. B., MORALES, M. M., FLOTTE, T. R., MCGRATH-MORROW, S. A., GUGGINO, W. B. & ZEITLIN, P. L. (1995). CIC-2: a developmentally dependent chloride channel expressed in the fetal lung and downregulated after birth. *Am J Respir Cell Mol Biol* **12**, 597-604.

- NEHRKE, K., ARREOLA, J., NGUYEN, H. V., PILATO, J., RICHARDSON, L., OKUNADE, G., BAGGS, R., SHULL, G. E. & MELVIN, J. E. (2002). Loss of hyperpolarization-activated Cl<sup>-</sup> current in salivary acinar cells from *Clcn2* knockout mice. *J Biol Chem* **277**, 23604-23611.
- NIEMEYER, M. I., YUSEF, Y. R., CORNEJO, I., FLORES, C. A., SEPULVEDA, F. V. & CID, L. P. (2004). Functional evaluation of human CIC-2 chloride channel mutations associated with idiopathic generalized epilepsies. *Physiol Genomics* **19**, 74-83.
- NOBILE, M., PUSCH, M., RAPISARDA, C. & FERRONI, S. (2000). Single-channel analysis of a CIC-2-like chloride conductance in cultured rat cortical astrocytes. *FEBS Lett* **479**, 10-14.
- PROTOPOPOV, A. I., GIZATULLIN, R. Z., VOROBIEVA, N. V., PROTOPOPOVA, M. V., KISS, C., KASHUBA, V. I., KLEIN, G., KISSELEV, L. L., GRAPHODATSKY, A. S. & ZABAROVSKY, E. R. (1996). Human chromosome 3: high-resolution fluorescence in situ hybridization mapping of 40 unique NotI linking clones homologous to genes and cDNAs. *Chromosome Res* **4**, 443-447.
- RENZ-POLSTER, H., KRAUTZIG, S. & BRAUN, J. (2004). *Basislehrbuch Innere Medizin*. Elsevier GmbH, München.
- RUDZINSKA, M. A., TRAGER, W. & BRAY, R. S. (1965). Pinocytotic uptake and the digestion of hemoglobin in malaria parasites. *J Protozool* **12**, 563-576.
- SAARI, J. T. & BECK, J. S. (1974). Probability density function of the red cell membrane permeability coefficient. *Biophys J* **14**, 33-45.
- SAIKI, R. K., GELFAND, D. H., STOFFEL, S., SCHARF, S. J., HIGUCHI, R., HORN, G. T., MULLIS, K. B. & ERLICH, H. A. (1988). Primer-directed enzymatic amplification of DNA with a thermostable DNA polymerase. *Science* **239**, 487-491.
- SANDER, T., SCHULZ, H., SAAR, K., GENNARO, E., RIGGIO, M. C., BIANCHI, A., ZARA, F., LUNA, D., BULTEAU, C., KAMINSKA, A., VILLE, D., CIEUTA, C., PICARD, F., PRUD'HOMME, J. F., BATE, L., SUNDQUIST, A., GARDINER, R. M., JANSSEN, G. A., DE HAAN, G. J., KASTELEIJN-NOLST-TRENITE, D. G., BADER, A., LINDHOUT, D., RIESS, O., WIENKER, T. F., JANZ, D. & REIS, A. (2000). Genome search for susceptibility loci of common idiopathic generalised epilepsies. *Hum Mol Genet* **9**, 1465-1472.
- SANGER, F., NICKLEN, S. & COULSON, A. R. (1977). DNA sequencing with chain-terminating inhibitors. *Proc Natl Acad Sci U S A* **74**, 5463-5467.
- SCHWIEBERT, E. M., CID-SOTO, L. P., STAFFORD, D., CARTER, M., BLAISDELL, C. J., ZEITLIN, P. L., GUGGINO, W. B. & CUTTING, G. R. (1998). Analysis of CIC-2

channels as an alternative pathway for chloride conduction in cystic fibrosis airway cells. *Proc Natl Acad Sci U S A* **95**, 3879-3884.

- SHERMAN, I. W. (1983). Metabolism and surface transport of parasitized erythrocytes in malaria. *Ciba Found Symp* **94**, 206-221.
- SIK, A., SMITH, R. L. & FREUND, T. F. (2000). Distribution of chloride channel-2-immunoreactive neuronal and astrocytic processes in the hippocampus. *Neuroscience* **101**, 51-65.
- SILFEN, J., YANAI, P. & CABANTCHIK, Z. I. (1988). Bioflavonoid effects on in vitro cultures of *Plasmodium falciparum*. Inhibition of permeation pathways induced in the host cell membrane by the intraerythrocytic parasite. *Biochem Pharmacol* **37**, 4269-4276.
- SMIRNOVA, I., MANN, N., DOLS, A., DERKX, H. H., HIBBERD, M. L., LEVIN, M. & BEUTLER, B. (2003). Assay of locus-specific genetic load implicates rare Toll-like receptor 4 mutations in meningococcal susceptibility. *Proc Natl Acad Sci U S A* **100**, 6075-6080.
- STAINES, H. M., ELLORY, J. C. & KIRK, K. (2001). Perturbation of the pump-leak balance for Na(+) and K(+) in malaria- infected erythrocytes. *Am J Physiol Cell Physiol* **280**, C1576-1587.
- STAINES, H. M., POWELL, T., ELLORY, J. C., EGEE, S., LAPAIX, F., DECHERF, G., THOMAS, S. L., DURANTON, C., LANG, F. & HUBER, S. M. (2003). Modulation of whole-cell currents in *Plasmodium falciparum*-infected human red blood cells by holding potential and serum. *J Physiol* **552**, 177-183.
- SYLLA, E. H., KUN, J. F. & KREMSNER, P. G. (2000). Mosquito distribution and entomological inoculation rates in three malaria-endemic areas in Gabon. *Trans R Soc Trop Med Hyg* **94**, 652-656.
- TANABE, K., KAGEYAMA, K. & TAKADA, S. (1986). An increase in water content of mouse erythrocytes infected with *Plasmodium yoelii*. *Trans R Soc Trop Med Hyg* **80**, 546-548.
- THIEMANN, A., GRUNDER, S., PUSCH, M. & JENTSCH, T. J. (1992). A chloride channel widely expressed in epithelial and non-epithelial cells. *Nature* **356**, 57-60.
- VERLOO, P., KOCKEN, C. H., VAN DER WEL, A., TILLY, B. C., HOGEMA, B. M., SINAASAPPEL, M., THOMAS, A. W. & DE JONGE, H. R. (2004). *Plasmodium falciparum*-activated chloride channels are defective in erythrocytes from cystic fibrosis patients. *J Biol Chem* **279**, 10316-10322.

WAGNER, M. A., ANDEMARIAM, B. & DESAI, S. A. (2003). A two-compartment model of osmotic lysis in *Plasmodium falciparum*-infected erythrocytes. *Biophys J* **84**, 116-123.

ZHANG, R., EVANS, G., ROTELLA, F. J., WESTBROOK, E. M., BENO, D., HUBERMAN, E., JOACHIMIAK, A. & COLLART, F. R. (1999). Characteristics and crystal structure of bacterial inosine-5'-monophosphate dehydrogenase. *Biochemistry* **38**, 4691-4700.

# 7 Appendix

## 7.1 Acknowledgment

First I would like to thank Prof. Dr. Florian Lang for giving me the opportunity to carry out this work in the Institute of Physiology, University of Tübingen.

I would also like to thank PD Dr. Jürgen F. J. Kun for all the support and guidance during my work with him and for his nice way of making one laugh.

I wish to thank Birgitta Noll for her patient and excellent instructions in practical work, which were very valuable, especially at the beginning of this study.

I am especially grateful to Andrea Weierich for her supervision during my stay at the Department of Human Parasitology, University of Tübingen.

I'd like to thank my supervisor PD Dr. Stephan Huber who helped me so much with my work and guided me with his way of positive thinking.

And last but not least I would like to thank my family for their great support throughout my studies and Anne Fritz for her helpful advice.

## 7.2 Curriculum Vitae

### Personal dates:

Name of birth: Jochen Paul  
Place of birth: Friedrichshafen (Germany)  
Date of birth: 12. September 1978  
Nationality: german

### Education:

1985 – 1989 Elementary school in Ravensburg  
1989 – 1998 Albert-Einstein-Gymnasium Ravensburg  
(High School)  
1998 Abitur (Senior High School Degree)  
Aug. 1998 – Aug. 1999 Civilian Service at the German Red Cross  
October 1999 Study of Medicine at the Eberhard Karls  
Universität Tübingen  
October 2001 Study of Sports Science at the Eberhard Karls  
Universität Tübingen  
(Dual study of Medicine and Sport Science in  
Tübingen)  
February – July 2003 Study at the University of Queensland in  
Brisbane, Australia (Human Movement)  
June 2005 Bachelor of Arts in Sports Science  
(Health management)  
since October 2005 Study of Medicine at the Technische  
Universität München  
26.10.2006 Third State Examination at the TU München